Defence Research and Development Canada
Recherche et développement pour la défense Canada

On the Receiver Operating Characteristics of Adaptive Radar Detectors

Christoph H. Gierull

Defence R&D Canada – Ottawa

Technical Memorandum
DRDC Ottawa TM 2013-117
December 2013

Canada

On the Receiver Operating Characteristics of Adaptive Radar Detectors

Christoph H. Gierull
Defence R&D Canada – Ottawa

Defence R&D Canada – Ottawa
Technical Memorandum
DRDC Ottawa TM 2013-117
December 2013

Principal Author

Original signed by Christoph H. Gierull

Christoph H. Gierull

Approved by

Original signed by Anthony Damini

Anthony Damini
Acting Head/Radar Sensing & Exploitation Section

Approved for release by

Original signed by Chris McMillan

Chris McMillan
Chair/Document Review Panel

Abstract

Aim of this technical memorandum is to analytically derive the probability of detection (vrs the probability of false alarms) of two variants of a square-law based adaptive radar detector when the target signal is buried in colored interference and when the filter vector to suppress the interference is not constant (i.e. unknown asymptotic covariance matrix) but a random vector itself. The filter or weight vector is assumed to be estimated via either Sample Matrix Inversion (SMI), Loaded SMI (LSMI) or Projection Techniques, such as Eigen-Vector Projection (EVP), Hung-Turner Projection (HTP) or Matrix Transformation based Projections (MTP), based on a limited number of statistical independent secondary training data. The analysis is based on a homogeneous, i.e. Gaussian, stationary clutter plus noise assumption. Target signals comprise different fluctuating RCS models as well as a constant deterministic model. The test statistic provides for the summation of several independent cells ('looks') to improve detection performance whereby the target must not necessarily be present in each cell. Although the analyzed detectors may not directly be applicable, the provided analytical analysis permits an analytical comparison of the various adaptive weights estimation techniques. In this sense it is an extension of the work presented in a previous technical memorandum [1] and its results and conclusions reflect an intermediate step towards unifying quantitative assessment of more advanced detectors such as the Adaptive Matched Filter (AMF) among others. The capability and usefulness of the presented equations are demonstrated based on numerical examples with a variety of different radar parameter settings.

Résumé

L'objectif de ce document technique est de calculer analytiquement la probabilité de détection (contre la probabilité de fausse alarme) de deux variantes d'un détecteur radar adaptatif quadratique lorsque le signal cible est masqué dans du brouillage de couleur et lorsque le vecteur de filtrage utilisé pour éliminer le brouillage n'est pas constant (c.-à-d. qu'on a une matrice de covariance asymptotique inconnue), mais un vecteur qui est lui-même aléatoire. On suppose que le vecteur de filtre ou de pondération est estimé soit par inversion de matrice d'échantillons (SMI), par SMI avec charge (LSMI) ou par des techniques de projection, tels que la projection de vecteur propre (EVP), la projection de type Hung-Turner (HTP) ou les projections basées sur des transformations de matrices (MTP), en se basant sur un nombre limité de données statistiques d'apprentissage secondaires indépendantes. L'analyse est basée sur l'hypothèse de la présence de fouillis et de bruit homogènes, c'est-à-dire statiques et gaussiens. Les signaux des cibles sont traités par divers modèles RCS fluctuants ainsi qu'avec un modèle déterministe constant. Les valeurs statistiques de test correspondent à la sommation de plusieurs cellules indépendantes (" visées ") qui sert

à améliorer les performances de détection alors que la cible n'est pas nécessairement présente dans chaque cellule. Bien que les détecteurs analysés puissent ne pas être directement applicables, l'analyse fournie permet une comparaison analytique des diverses techniques d'estimation des poids adaptatifs. En ce sens, il s'agit d'une extension du travail présenté dans une note technique précédente [1] et ses résultats et conclusions reflètent une étape intermédiaire vers l'évaluation quantitative unificatrice de détecteurs plus avancés, notamment le filtre adapté adaptatif (AMF). La capacité et l'utilité des équations présentées sont mises en évidence à partir d'exemples numériques avec une diversité de différents paramètres radar.

Executive summary

On the Receiver Operating Characteristics of Adaptive Radar Detectors

Christoph H. Gierull; DRDC Ottawa TM 2013-117; Defence R&D Canada – Ottawa; December 2013.

Background: Canada's Forces (CF) deploy Ground Moving Target Indication (GMTI) radars on their CP-140 maritime patrol aircrafts and on the remote sensing satellite RADARSAT-2 to operationally monitor the country's vast ocean approaches. In addition, the Department of National Defence (DND) is investing in the development of modern multi-functional phased array antennas for deployment on their future naval platforms, air surveillance (air-defense) radars and over-the-horizon radar systems. To be effective, these systems need to employ Space-Time Adaptive Processing (STAP) and adaptive beamforming techniques to reduce strong detrimental interference (clutter, jammer), which otherwise will significantly compromise their performance. Both applications have in common that the filter to suppress the undesired interference exploits the knowledge of the mutual cross-correlation between all receiver channels in form of the covariance matrix. If the covariance matrix is a priori known, the filter is constant and the resulting performance has been investigated and well reported in the literature. In practice, however, the covariance matrix is not known and hence the filter vector must be estimated from a limited number of statistically independent secondary measurements, which is then subsequently applied to the primary data under consideration. Since there exist several different estimation techniques with varying statistical properties, the theoretical performance analysis is challenging. Most of the previous work has been limited to the investigation of either simplified loss factors due to mathematical tractability, or to one classical (but not necessary optimum) estimation technique, or has been restricted to one particular target signal model.

Principal results: This memorandum presents a novel unifying theoretical analysis to examine the performance of a certain class of adaptive Constant False Alarm Rate (CFAR) detectors in a homogeneous, Gaussian interference environment. In particular, the analysis comprises several well-known estimation techniques for the suppression filter, deterministic and random target signal models, arbitrary channel sizes, selectable dimensionality of the interference as well as incoherent summing ('multi-looking') of independent test cells. It provides closed form analytical expressions that permit numerical computation of the complete Receiver Operating Characteristics (ROC), i.e. the probability of target detectability versus a varying false alarm rate with an arbitrary high accuracy. The utility and usefulness of the

theoretical work has been demonstrated with examples featuring a variety of different parameter settings and processing methods. The numerical tools have been proven to be flexible, efficient and robust.

Significance of results: The main objective of this memorandum is a step towards an overarching analytical framework that allows prediction of the performance of adaptive detectors under the realistic assumption that the filter vector is unknown and must be estimated using auxiliary measurements. The analysis provides for the first time the opportunity to directly compare the capabilities of various estimation techniques and therewith to predict which technique will yield superior results under some practically relevant conditions, including different target signal models. Another substantial contribution of this report is to provide a radar designer or operator with tools with whom they can determine how much training data are necessary to obtain, for instance, a 90% detection level compared to the optimum value (hypothetically achievable if the covariance matrix was known). Since it depends strongly on the desired false alarm rate, this is a much more practical and meaningful metric than the commonly used average loss of signal-to-noise-plus-interference (SNIR) power ratio. The presented algorithms have already been successfully incorporated into theoretical performance analysis for the Multi-Sensor Data Fusion project at DRDC Ottawa.

Future work: The most important extension of the presented analysis concerns the inclusion of practically more relevant detectors such as the Adaptive Matched Filter (AMF) or the Generalized Likelihood Ratio Test (GLRT) [2] for which the detection probabilities have been calculated only for SMI [3, 4] but not for the advanced weights like LSMI/EVP. Another open problem relates to non-ideal conditions such as that the true target direction (for adaptive beamforming) or true velocity (for STAP processing) are not known. Therefore, the true target or signal vector $\boldsymbol{s}$ might not align with the assumed steering vector $\boldsymbol{d}$; In other words the case that the signal impinges on the array from a slightly different direction from that into which the antenna was steered. The implications of this mismatch on the statistical properties have originally been investigated by Boroson [5, 2] see also [4]. The proposed theoretical approach in these papers is supposed to be directly applicable to the problem at hand in this report.

Sommaire

On the Receiver Operating Characteristics of Adaptive Radar Detectors

Christoph H. Gierull ; DRDC Ottawa TM 2013-117 ; R & D pour la défense Canada – Ottawa ; décembre 2013.

Introduction : Les Forces canadiennes (FC) déploient des radars GMTI (de détection de cibles mobiles au sol) sur leurs avions de patrouille maritime CP-140 et sur le satellite de télédétection RADARSAT-2 pour surveiller les vastes zones d'approche océanique du pays. En outre, le ministère de la Défense nationale (MDN) investit dans le développement d'antennes à balayage électronique multifonctionnelles modernes destinées à être déployées sur ses futures plateformes navales, à effectuer de la surveillance radar et à servir avec les systèmes radar aériens transhorizon (pour la défense aérienne). Pour être efficaces, ces systèmes doivent employer le traitement adaptatif spatio-temporel (STAP) et des techniques de formation de faisceaux adaptatifs pour réduire le fort brouillage nuisible (fouillis, brouilleurs), qui autrement compromet considérablement leur performance. Les deux applications ont en commun que le filtre qui supprime le brouillage indésirable exploite la connaissance de la corrélation mutuelle entre tous les canaux de réception sous la forme d'une matrice de covariance. Si la matrice de covariance est connue a priori, le filtre est constant, et la performance résultante a été étudiée et bien documentée dans la littérature. En pratique toutefois, la matrice de covariance n'est pas connue et le vecteur filtre doit donc être estimé à partir d'un nombre limité de mesures secondaires statistiquement indépendantes, qui seront ensuite appliquées aux données primaires à l'étude. Comme il existe plusieurs techniques d'estimation différentes ayant différentes propriétés statistiques, l'analyse de la performance théorique est difficile. La plupart des travaux antérieurs ont été limités à l'étude de facteurs d'affaiblissement simplifiés en raison de questions de résolubilité mathématique ou à une technique d'estimation classique (mais pas nécessairement optimale), ou ont été limités à un modèle particulier de signal de cible.

Résultats principaux : Cette note présente une analyse théorique unificatrice et novatrice afin d'examiner la performance d'une certaine catégorie de détecteurs adaptatifs de taux de fausse alarme constant (TFAC) dans un environnement de brouillage gaussien homogène. En particulier, l'analyse fait appel à plusieurs techniques bien connues d'estimation pour le filtre de suppression, des modèles de signaux cibles déterministes et aléatoires, des tailles de canal arbitraires, des choix d'intensité de brouillage ainsi que la sommation incohérente (" multi-visées ") de cellules de test indépendantes. Il fournit des expressions analytiques fermées qui permettent le cal-

cul numérique des caractéristiques de fonctionnement du récepteur (ROC) complètes, c'est-à-dire la probabilité de détectabilité de la cible par rapport à un taux de fausses alarmes variant avec une grande précision arbitraire. L'utilité du travail théorique a été démontrée par des exemples comportant une diversité de différents paramètres et méthodes de traitement. La polyvalence, l'efficacité et la robustesse des outils numériques ont été prouvées.

Importance des résultats : L'objectif principal de cette note est de progresser vers un cadre analytique global qui permettra de prédire la performance des détecteurs adaptatifs avec l'hypothèse réaliste que le vecteur filtre est inconnu et doit être estimé à partir de mesures auxiliaires. Cette analyse fournit pour la première fois la possibilité de comparer directement les capacités des différentes techniques d'estimation et ainsi de prédire quelle technique donnera des résultats supérieurs dans certaines conditions pratiques pertinentes, y compris en présence de différents modèles de signaux de cible. Une autre contribution importante de ce rapport est de fournir à un concepteur ou opérateur de radar des outils avec lesquels ils pourront déterminer la quantité de données d'apprentissage nécessaire pour obtenir, par exemple, un niveau de détection de 90 % par rapport à la valeur optimale (hypothétiquement réalisable si la matrice de covariance était connue). Comme cela dépend fortement du taux de fausse alarme souhaité, c'est une mesure beaucoup plus pratique et significative de l'affaiblissement moyen calculé avec le rapport signal sur bruit plus brouillage (SNIR) couramment utilisé. Les algorithmes présentés ont déjà été incorporés avec succès dans l'analyse de la performance théorique pour le projet de fusion de données multi-capteurs à RDDC Ottawa.

Perspectives : L'extension la plus importante de l'analyse présentée concerne l'inclusion des détecteurs pratiquement plus pertinents, tels que le filtre adapté adaptatif (AMF) ou le test de rapport de vraisemblance généralisé (GLRT) [2] pour lesquels les probabilités de détection ont été calculées uniquement pour la SMI [3, 4], mais pas pour les pondérations avancées qu'on peut obtenir par LSMI/EVP. Un autre problème concerne les conditions non idéales comme l'ignorance de la vraie direction de la cible (pour la formation adaptative de faisceau) ou sa vitesse vraie (pour le traitement STAP). Par conséquent, la vraie valeur du vecteur de cible ou de vitesse s pourrait ne pas correspondre au vecteur de direction supposée d ; en d'autres termes, c'est un cas où le signal arrive à l'antenne réseau à partir d'une direction légèrement différente de celle dans laquelle l'antenne a été dirigée. Les conséquences de ce décalage des propriétés statistiques ont été initialement étudiées par Boroson [5, 2] (voir aussi [4]). L'approche théorique proposée dans ces documents devrait être directement applicable au problème traité dans le présent rapport.

Table of contents

List of figures

List of tables

List of variables

η	Threshold to be computed via (27) for given constant false alarm rate (CFAR), see equation (3), page 1
ν	Adaptive beamformer technique indicator, $\nu \in \{N-1, M\}$, see equation (23), page 5
$\boldsymbol{d}$	Target DOA or steering vector, see equation (8), page 2
K	Number of secondary training samples to estimate the covariance matrix $\mathbf{R}$, $K \geq N$, statistically independent from n primary samples, page 2
L	Number of looks containing the target, $1 \leq L \leq n$, page 2
M	Dimension of the clutter subspace, $M < N$, page 3
N	Number of channels, see equation (1), page 1
n	Number of looks (incoherent sum used in detector), page 1
s	Random target RCS model indicator, $s \in \{1, L, 2, 2L, \infty\}$, see equation (42), page 9

1 Introduction

Adaptive multi-channel or sensor detection techniques and algorithms are nowadays widely used for interference suppression in active radar applications such as control of the antenna pattern in adaptive arrays (also called adaptive beamforming) [4] or in post-Doppler Space-Time Adaptive Processing (STAP) for Ground Moving Target Indication (GMTI) under severe clutter conditions [6, 7]. If the Gaussian interference, or more precisely the interference covariance matrix, is known, the maximization of the Signal-to-Noise-plus-Interference Ratio (SNIR) is equivalent to the maximization of the detection probability P_{d} for a fixed false alarm rate [6]. The adaptive processor linearly combines the elements of the data snapshot $\boldsymbol{Z} = [Z_1, \ldots, Z_N]$ yielding a scalar output

$$\bar{T} = \boldsymbol{u}^* \boldsymbol{Z}. \tag{1}$$

where N is the number of channels, and $\boldsymbol{u}$ denotes the weight or filter vector. The SNIR of this filter output for a given (expected) target signal $\boldsymbol{s}$ is

$$\mathrm{SNIR} := \kappa = \frac{\mathsf{E}\,|\boldsymbol{u}^* \boldsymbol{s}|^2}{\mathsf{E}\,\boldsymbol{u}^* \boldsymbol{W}\,\boldsymbol{W}^* \boldsymbol{u}}, \tag{2}$$

in which $\mathbf{R} = \mathsf{E}\,\boldsymbol{W}\,\boldsymbol{W}^*$ is the interference covariance matrix. E denotes the expectation operator. Assuming the interference comprises of a clutter component $\boldsymbol{C}$ and an independent thermal noise component $\boldsymbol{N}$, and under the Gaussian assumption for the interference data $\boldsymbol{W} = \boldsymbol{C} + \boldsymbol{N} \sim \mathcal{N}_N^{\mathbb{C}}(\boldsymbol{0}, \mathbf{R})$ with $\mathbf{R} = \mathbf{R}_{\boldsymbol{C}} + \mathbf{R}_{\boldsymbol{N}}$, the optimum detector follows from a Likelihood-Ratio-Test (LRT) [6]

$$|\bar{T}|^2 \gtrless \eta, \tag{3}$$

where η denotes the detection threshold. This threshold is set to discriminate between one of the two hypotheses

$$\mathfrak{H}: \quad \boldsymbol{Z} = \boldsymbol{C} + \boldsymbol{N} \quad \text{(interference alone)} \tag{4}$$

$$\mathfrak{A}: \quad \boldsymbol{Z} = \boldsymbol{S} + \boldsymbol{C} + \boldsymbol{N} \quad \text{(interference plus target)} \tag{5}$$

for a given probability of false alarms P_{fa}.

If n independent snapshots $\boldsymbol{Z}_k$ for $k = 1, \ldots, n$ are available, which possess the same statistical properties, the test becomes the incoherent sum [8]

$$\bar{T} = \sum_{k=1}^{n} |\boldsymbol{u}^* \boldsymbol{Z}_k|^2 \gtrless \eta. \tag{6}$$

This is for instance the case in SAR-GMTI application when the target spread over multiple image resolution cells, or when multilook GMTI processing is applied,

i.e. when the entire available frequency bands are divided into subbands that are incoherently added [9]. Multilook processing is commonly applied in order to reduce speckle variation in the SAR image causing graininess. The parameter n will be called number of looks from here onwards in line with the SAR example. Note, for the following analysis it is not required that the target is present in each cell, i.e. we introduce an additional parameter L describing the number of looks actually containing the target with $1 \leq L \leq n$.

Without loss of generality, the test can be normalized to the expected value under the hypothesis $\mathfrak{H}$, i.e.

$$\mathsf{E}\,\bar{T}_{\mathfrak{H}} = \sum_{k=1}^{n} \boldsymbol{u}^* \,\mathsf{E}\,(\boldsymbol{Z}_k \boldsymbol{Z}_k^*)\,\boldsymbol{u} = n\boldsymbol{u}^*\mathbf{R}\boldsymbol{u}, \tag{7}$$

so that

$$T := \frac{\bar{T}}{n\boldsymbol{u}^*\mathbf{R}\boldsymbol{u}} = \frac{1}{n}\sum_{k=1}^{n} \frac{|\boldsymbol{u}^*\boldsymbol{Z}_k|^2}{\boldsymbol{u}^*\mathbf{R}\boldsymbol{u}}, \tag{8}$$

with $\mathsf{E}\,T = 1$.

As mentioned before, for a signal vector $\boldsymbol{s} = \sigma_t \boldsymbol{d}$, the P_d is essentially determined by the achievable SNIR $\kappa = \sigma_t^2 \frac{|\boldsymbol{u}^*\boldsymbol{d}|^2}{\boldsymbol{u}^*\mathbf{R}\boldsymbol{u}}$; hence maximizing κ will maximize P_d. The common amplitude σ_t determines the related Signal-to-Noise Ratio (SNR), a function of the target's RCS, and the vector $\boldsymbol{d}$ is usually denoted as steering or Direction-Of-Arrival (DOA) vector. The weight vector to maximize the SNIR is well known to be

$$\boldsymbol{u}_\mathrm{opt} = \alpha\mathbf{R}^{-1}\boldsymbol{d}, \tag{9}$$

[4, 6] in which α is an arbitrary constant resulting in the optimum SNIR

$$\kappa_\mathrm{opt} = \sigma_t^2 \boldsymbol{d}^*\mathbf{R}^{-1}\boldsymbol{d}. \tag{10}$$

The SNIR loss function has been defined as

$$\kappa_l = \frac{\kappa}{\kappa_\mathrm{opt}} = \frac{|\boldsymbol{u}^*\boldsymbol{d}|^2}{\boldsymbol{u}^*\mathbf{R}\boldsymbol{u}} \frac{1}{\boldsymbol{d}^*\mathbf{R}^{-1}\boldsymbol{d}}. \tag{11}$$

In reality, however, the covariance matrix is not known and must be estimated. This estimation is conventionally done using K independent secondary training samples $\mathbf{X} = [\boldsymbol{X}_1, \ldots, \boldsymbol{X}_K]$ for the interference (i.e. in the absence of a target) that possess the same statistical properties as the primary data, i.e. $\boldsymbol{X}_k \sim \mathcal{N}_N^{\mathbb{C}}(\boldsymbol{0}, \mathbf{R})$. In their classic paper, Reed, Brennan and Mallet [10] proposed to replace $\mathbf{R}$ with its Maximum Likelihood Estimation (MLE)

$$\hat{\mathbf{R}} = \frac{1}{K}\mathbf{X}\mathbf{X}^* = \frac{1}{K}\sum_{k=1}^{K} \boldsymbol{X}_k \boldsymbol{X}_k^* \qquad K \geq N. \tag{12}$$

Please note that this approach is rather ad hoc and heuristically motivated and by no means satisfying an optimization criterion. In this memorandum, random vectors are capitalized and slanted while matrices are capitalized using a straight font. Their corresponding realizations are written in small letters.

Inserting

$$\hat{\boldsymbol{U}}_{\mathrm{SMI}} = \hat{\mathbf{R}}^{-1}\boldsymbol{d} \tag{13}$$

into (11) yields the scalar random variable

$$\mathcal{K}_l = \frac{|\boldsymbol{d}^*\hat{\mathbf{R}}^{-1}\boldsymbol{d}|^2}{\boldsymbol{d}^*\hat{\mathbf{R}}^{-1}\mathbf{R}\hat{\mathbf{R}}^{-1}\boldsymbol{d}}\,\frac{1}{\boldsymbol{d}^*\mathbf{R}^{-1}\boldsymbol{d}}, \tag{14}$$

which has been shown to follow a beta-distribution with $2(K-N+2), 2(N-1)$ degrees of freedom [10]. This method has been called Sample Matrix Inversion (SMI). Many researchers have used the expectation of (14) to determine the average number of training samples, $K_{3\mathrm{dB}} = 2N-3$, required to reach a 3dB SNIR loss, e.g. [11]. However, it has been realized that considering only the mean is not sufficient as it neglects the impact of the variability of the random variable. Nitzberg [12] proposed a more suitable performance metric for SMI, the detection loss, for which he showed that (in contrast to the mean value) it depends also on the false alarm rate, the number of channels as well as the secondary sample size. Wang and Cai [13] went a step further and analyzed the probability of detection of the square-law detector when the weights are estimated via SMI. Presumably for mathematical tractability, however, they limited their derivation to Swerling target scenarios that are statistically independent from the interference [14].

Instead of inverting the Sample Covariance Matrix (SCM), Carlson [15] showed that it is advantageous in most cases[1] to add a small constant to the SCM prior to inversion:

$$\hat{\boldsymbol{U}}_{\mathrm{LSMI}} = \alpha\left(\frac{1}{K}\sum_{k=1}^{K}\boldsymbol{X}_k\boldsymbol{X}_k^* + \delta\mathbf{I}\right)^{-1}\boldsymbol{d}. \tag{15}$$

This addition compresses and smoothes the usually strongly fluctuating noise eigenvalues which have a detrimental effect on the SNIR loss [4, 16]. The probability density function (pdf) of the so-called Loaded SMI (LSMI) has originally been derived by [17], see also [16]. $\mathcal{K}_l$ for the LSMI follows also a beta-distribution but with $2(K-M-1), 2M$ degrees of freedom. The number of required secondary data is significantly reduced to $K_{3\mathrm{dB}} = 2M$, when M denotes the number of large interference/clutter eigenvalues which can be significantly smaller than the number of channels N.

[1] Particularly when the number of samples is small and especially smaller than the number of channels which leads to a non-invertible covariance matrix.

Arguably the best known so-called projection technique is the Eigen Vector based Projection (EVP) [4] that completely avoids the small eigenvalues:

$$\hat{\boldsymbol{U}}_{\mathrm{EVP}} = \alpha \left(\mathbf{I} - \mathbf{E}_C \mathbf{E}_C^*\right) \boldsymbol{d}, \tag{16}$$

where $\hat{\mathbf{R}} = [\mathbf{E}_C \mathbf{E}_N] \Lambda [\mathbf{E}_C \mathbf{E}_N]^*$ denotes the eigenvalue decomposition of the sample covariance matrix and $\mathbf{E}_C \in \mathbb{C}^{N \times M}$ represent the estimated clutter subspace. It has been shown that the statistical properties of EVP are under some mild conditions are identical to that of LSMI [18]. In order to avoid the computational expense associated with an eigenvector decomposition of a potentially large covariance matrix, many eigenvector-free techniques have been proposed in the past. A classical representative of this class of techniques is the Hung-Turner Projection (HTP) developed at DRDC Ottawa, in which the projection matrix is directly generated by the set of secondary samples [19]. The statistical properties of the HTP have been derived in [20] using fundamental results presented in [17][2]. An economically most favorable technique in terms of computational load, called Matrix Transformation based Projection (MTP), which achieves optimal performance (i.e. nearly identical to LSMI/EVP) was introduced in [21]. A comprehensive summary of these kind of techniques can be found in [16] and in English in [22]. A statistical analysis of projection techniques for small sample sizes was provided in [23].

The objective of this memorandum is to provide a generalized and unifying analysis, comprising the different estimation techniques of the filter vector, of the operationally relevant full Receiver Operator Characteristics (ROC) for the classic class of square-law detectors [8, 24] rather than the SNIR loss or detection loss factors. Although the two analyzed detectors are not the most practical relevant, their thorough assessment is an important step towards a unifying theoretical framework which eventually shall comprise all practical detectors and advanced adaptive weight vectors. For instance. the presented derivations include a parameterized target model covering all fluctuating Weinstein or Swerling cases as well as the constant (deterministic) RCS model. In addition to previous work the analysis includes incoherent multilooking at which the target must not necessarily be present in each cell. Last but not least, through a single parameter it permits the performance comparison of SMI on one hand and the LSMI/EVP on the other hand. The memorandum presents analytical closed form expressions leading to efficient numerical recipes to compute the probability of detection with an arbitrarily small error, which have been shown to work robustly for radar systems consisting of several hundreds channels processing several hundred secondary data. The theoretical foundation of this work is based on the work by Mitchell and Walker [25] and Shnidman [26, 27], see also [1]. For completeness sake it should be mentioned that alternative detectors have been suggested for instance by Kelly [28] and Robey et. al. [29], and were statistically analyzed in depth by Richmond [3].

[2]Some additional analysis for the HTP is being presented in this report, see Annexes B and C.

2 Detector statistics

Suppose that the decision whether or not a moving target is present in the multi-channel data is based on the square-law test

$$\begin{aligned} \bar{T} &= \|\mathbf{Z}^* \boldsymbol{U}\|^2 = \boldsymbol{U}^* \mathbf{Z}\mathbf{Z}^* \boldsymbol{U} \\ &= \sum_{k=1}^{n} |\, \boldsymbol{U}^* \boldsymbol{Z}_k|^2 \,. \end{aligned} \tag{17}$$

As extension to the test in (6), the weight vector intended to suppress the interference $\boldsymbol{U}$ is not deterministic and known but a random vector of size $N \times 1$ itself. The random matrix $\mathbf{Z}$ of size $n \times N$ contains as columns n statistically independent Gaussian primary data vectors, with

$$\boldsymbol{Z}_k = \boldsymbol{S}_k + \boldsymbol{W}_k, \qquad \boldsymbol{W}_k = \boldsymbol{C}_k + \boldsymbol{N}_k \sim \mathcal{N}_N^{\mathbb{C}}\left(\boldsymbol{0}, \mathbf{R}\right), \tag{18}$$

for $k = 1, \ldots, n$, where $\mathbf{R} = \mathbf{R}_{\boldsymbol{C}} + \mathbf{R}_{\boldsymbol{N}}$ denotes the clutter plus noise covariance matrix and $\boldsymbol{S}$ denotes a potential moving target signal. According to equation (23) in [1], assuming homogeneous clutter for which $\Delta = \delta = 1$, the conditional probability density function (pdf) of the test (17) for constant target signal $\boldsymbol{S} = \boldsymbol{s}$ and constant weight $\boldsymbol{U} = \boldsymbol{u}$ reads

$$f_{(\bar{T}|\boldsymbol{S}=\boldsymbol{s},\boldsymbol{U}=\boldsymbol{u})}(\bar{t};\boldsymbol{s},\boldsymbol{u}) = \left(\frac{1}{\sigma^2}\right)^{\frac{n+1}{2}} \left(\frac{\bar{t}}{\omega}\right)^{\frac{n-1}{2}} \exp\left(-\frac{\bar{t}}{\sigma^2} - \omega\right) \mathrm{I}_{n-1}\left(2\sqrt{\omega\frac{\bar{t}}{\sigma^2}}\right)$$

with

$$\begin{aligned} \sigma^2 &= \boldsymbol{u}^* \mathbf{R} \boldsymbol{u}, \\ \omega &= L\frac{|\boldsymbol{u}^* \boldsymbol{s}|^2}{\sigma^2} = L\frac{|\boldsymbol{u}^* \boldsymbol{s}|^2}{\boldsymbol{u}^* \mathbf{R} \boldsymbol{u}} \\ \boldsymbol{s} &= \sigma_t \boldsymbol{d}, \end{aligned} \tag{19}$$

where the common amplitude σ_t determines the related Signal-to-Noise Ratio (SNR), mainly driven by the target's RCS, and the vector $\boldsymbol{d}$ is usually denoted as steering vector containing information on the target's across-track velocity component v_y or its bearing, and I_m denotes the Bessel function of the first kind of order m.

Let us re-write the variable ω as a linear function of the SNIR loss (11), i.e.

$$\omega = \underbrace{L\sigma_t^2\, \boldsymbol{d}^* \mathbf{R}^{-1} \boldsymbol{d}}_{a} \cdot \underbrace{\frac{|\boldsymbol{u}^* \boldsymbol{s}|^2}{\boldsymbol{u}^* \mathbf{R} \boldsymbol{u}} \frac{1}{\boldsymbol{d}^* \mathbf{R}^{-1} \boldsymbol{d}}}_{\kappa_l}, \tag{20}$$

with the new variable $a := L\sigma_t^2\, \boldsymbol{d}^*\mathbf{R}^{-1}\boldsymbol{d}$ so that (19) can be expressed as conditioned on fixed $A = a$ and $\mathcal{K}_l = \kappa_l$ rather than the weight vector itself, i.e.

$$f_{\bar{T}|A,\mathcal{K}_l}(t; a, \kappa_l, \sigma^2) = \left(\frac{1}{\sigma^2}\right)^{\frac{n+1}{2}} \left(\frac{\bar{t}}{a\kappa_l}\right)^{\frac{n-1}{2}} \exp\left(-\frac{\bar{t}}{\sigma^2} - a\kappa_l\right) \mathrm{I}_{n-1}\left(2\sqrt{a\kappa_l \frac{\bar{t}}{\sigma^2}}\right). \tag{21}$$

For notational simplicity we will omit the index l from here onwards. However, the conditional pdf still depends on σ^2, which is a function of $\boldsymbol{u}$. The key step in the provided analysis is to normalize the test appropriately so that the dependency on σ^2 in (21) disappears, and the unconditional pdf results from integrating over the two random variables A and $\mathcal{K}$. It will be shown that this can be achieved for instance by the following two normalizations:

$$a)\ T := \frac{\bar{T}}{n\, \boldsymbol{U}^*\mathbf{R}\,\boldsymbol{U}} \qquad \text{and} \qquad b)\ T := \frac{\bar{T}}{n\,|\,\boldsymbol{U}^*\boldsymbol{d}|^2}. \tag{22}$$

Observe that b) is a perfectly valid test that is strongly related to the AMF except for the square of the denominator, while a) is of a mere academic nature since the asymptotic covariance $\mathbf{R}$ was assumed unknown to begin with, and hence cannot appear in the denominator. Nevertheless, the analytical analysis and the derived closed form solutions for the performance metrics provide valuable insight into the relative comparison of various adaptive weight estimation techniques, which has not been established in the literature. Furthermore, this approach may also open the door to enable the derivation of closed form solutions for more practical detectors such as AMF and GLRT involving advanced adaptive weights.

For brevity we derive the P_{fa} and P_{d} in detail only for Test a) in the subsequent sections and in a much briefer form for Test b) in Annex D. The normalization for Test a) is reflected through

$$\begin{aligned} f_{T|A,\mathcal{K}}(t; a, \kappa) &= n\sigma^2 f_{\bar{T}|A,\mathcal{K}}(n\sigma^2 t; a, \kappa, \sigma^2) \\ &= n^{\frac{n+1}{2}} \left(\frac{1}{a\kappa}\right)^{\frac{n-1}{2}} t^{\frac{n-1}{2}}\, e^{-nt}\, e^{-a\kappa}\, \mathrm{I}_{n-1}\left(2\sqrt{na\kappa t}\right). \end{aligned} \tag{23}$$

In this memorandum we concentrate on the two distinct classes of adaptive weight estimators, SMI and LSMI/EVP/MTP, respectively as their statistical properties can be parameterized using a single parameter, i.e. the pdf of the SNIR loss random variable (14) containing the estimated filter vector

$$\mathcal{K} = \frac{|\,\hat{\boldsymbol{U}}^*\boldsymbol{d}|^2}{\hat{\boldsymbol{U}}^*\mathbf{R}\,\hat{\boldsymbol{U}}} \frac{1}{\boldsymbol{d}^*\mathbf{R}^{-1}\boldsymbol{d}} \tag{24}$$

is beta-distributed, $\sim \beta_{2(K-\nu+1),2\nu}$, with pdf

$$f_{\mathcal{K}}(\kappa) = \frac{\Gamma(K+1)}{\Gamma(\nu)\Gamma(K-\nu+1)}\,\kappa^{K-\nu}\,(1-\kappa)^{\nu-1} \qquad 0 < \kappa \leq 1, \tag{25}$$

in which the new parameter ν is used to indicate the applied estimation technique

Table 1: *Estimation Technique Selection Parameter*

Parameter ν	Method
$N-1$	SMI
M	LSMI/EVP/MTP

However it should be noted that any estimation technique for which a density function $f_{\mathcal{K}}(\kappa)$ exists, can be analytically investigated with regard to its achievable probability of detection, cf. (31). For instance in Annex C the P_{d} of the classical Hung-Turner Projection (HTP) method is derived using the newly found closed form expression of the pdf for $\mathcal{K}$ in Annex B.

3 Probability of false alarm

Setting $a = 0$ and using the result of Annex A in [16], the conditional pdf in absence of a target is given to under the assumption of homogeneous clutter with $\bar{\sigma}^2 = \sigma^2$

$$f_{(T|\mathcal{K})}(t;0,\kappa) = n^n \frac{t^{n-1}}{\Gamma(n)}\,e^{-nt}, \tag{26}$$

which does not depend on the weighting vector or κ respectively, and leads to the probability of false alarm P_{fa}

$$P_{\mathrm{fa}}(\eta) = \frac{\Gamma(n, n\eta)}{\Gamma(n)}, \tag{27}$$

where $\Gamma(\cdot,\cdot)$ denotes the incomplete gamma function [16].

4 Probability of detection

4.1 Deterministic target signal

4.1.1 Arbitrary number of channels

For a deterministic target, we can set $A = a \equiv \xi$ and yield for the conditional pdf in (21)

$$f_{(T|\mathcal{K})}(t;\kappa) = n^{\frac{n+1}{2}} \left(\frac{1}{\xi}\right)^{\frac{n-1}{2}} t^{\frac{n-1}{2}}\, e^{-nt} \left(\frac{1}{\kappa}\right)^{\frac{n-1}{2}} e^{-\xi\kappa}\, \mathrm{I}_{n-1}\left(2\sqrt{n\xi\kappa t}\right). \tag{28}$$

Using the power series representation for the Bessel function

$$\mathrm{I}_{n-1}\left(2\sqrt{n\xi\kappa t}\right) = \sum_{\mu=0}^{\infty} \frac{1}{\Gamma(\mu+1)\Gamma(n+\mu)} \left(\sqrt{n\xi\kappa t}\right)^{n-1+2\mu} \tag{29}$$

in (28) yields

$$f_{(T|\mathcal{K})}(t;\kappa) = \sum_{\mu=0}^{\infty} \frac{n^{n+\mu}\xi^{\mu}}{\Gamma(\mu+1)\Gamma(n+\mu)}\, t^{n+\mu-1} e^{-nt} \kappa^{\mu} e^{-\xi\kappa}. \tag{30}$$

Since

$$f_T(t) = \int_0^1 f_{(T|\mathcal{K})}(t;\kappa)\, f_{\mathcal{K}}(\kappa)\, d\kappa, \tag{31}$$

by using (25) we get for the test statistic

$$f_T(t) = \sum_{\mu=0}^{\infty} \frac{\Gamma(K+1)}{\Gamma(\mu+1)\Gamma(n+\mu)\Gamma(\nu)\Gamma(K-\nu+1)} \; n^{n+\mu}\xi^{\mu} t^{n+\mu-1} e^{-nt} \underbrace{\int_0^1 \kappa^{K-\nu+\mu}(1-\kappa)^{\nu-1}\, e^{-\xi\kappa}\, d\kappa}_{B(K-\nu+\mu+1,\nu)\,{}_1\mathrm{F}_1(K-\nu+\mu+1,K+\mu+1;-\xi)}, \tag{32}$$

where we have used the result in [30][p.343-3.383-1], and $B(a,b) = \frac{\Gamma(a)\Gamma(b)}{\Gamma(a+b)}$. Using (32) the probability of detection P_{d} can be computed to

$$\begin{aligned} P_{\mathrm{d}}(\eta, K) &= \int_{\eta}^{\infty} f_T(t)\, dt \\ &= \sum_{\mu=0}^{\infty} \frac{\Gamma(K+1)\Gamma(n+\mu, n\eta)}{\Gamma(\mu+1)\Gamma(n+\mu)\Gamma(\nu)\Gamma(K-\nu+1)} \xi^{\mu} \int_0^1 \kappa^{K-\nu+\mu}(1-\kappa)^{\nu-1}\, e^{-\xi\kappa}\, d\kappa \\ &= \sum_{\mu=0}^{\infty} \frac{\Gamma(n+\mu, n\eta)}{\Gamma(n+\mu)} \; \frac{\Gamma(K+1)B(K-\nu+\mu+1,\nu)}{\Gamma(\mu+1)\Gamma(\nu)\Gamma(K-\nu+1)} \\ &\qquad \times \xi^{\mu}\, {}_1\mathrm{F}_1\left(K-\nu+\mu+1, K+\mu+1; -\xi\right), \end{aligned} \tag{33}$$

where it has been used that the integral with respect to t evolves to an incomplete Gamma function:

$$\int_{\eta}^{\infty} t^{n+\mu-1} e^{-nt}\, dt = \frac{\Gamma(n+\mu, n\eta)}{n^{n+\mu}}. \tag{34}$$

Since ν appearing in the power under the integral in (32) is always $\in \mathbb{N}$, one can use the finite power series

$$(1-\kappa)^{\nu-1} = \sum_{j=0}^{\nu-1} \binom{\nu-1}{j} (-1)^j\, \kappa^j \tag{35}$$

to get a closed form solution for the integral

$$\sum_{j=0}^{\nu-1} \binom{\nu-1}{j} (-1)^j \underbrace{\int_0^1 \kappa^{K-\nu+\mu+j} e^{-\xi\kappa}\, d\kappa}_{\left(\frac{1}{\xi}\right)^{K-\nu+\mu+j+1} \gamma(K-\nu+\mu+j+1,\xi)}, \tag{36}$$

where $\binom{\cdot}{\cdot}$ is the binomial coefficient which can be expressed to

$$\binom{\nu-1}{j} = \frac{\Gamma(\nu)}{\Gamma(j+1)\Gamma(\nu-j)} = \prod_{l=1}^{j} \frac{\nu-j-1+l}{l}. \tag{37}$$

Using for instance the gamma-functions relationship in (37) the P_{d} can be computed via

$$P_{\mathrm{d}}(\eta) = \sum_{\mu=0}^{\infty} \sum_{j=0}^{\nu-1} (-1)^j \frac{\Gamma(K+1)\,\Gamma(n+\mu, n\eta)\,\gamma(K-\nu+\mu+j+1, \xi)}{\Gamma(\mu+1)\Gamma(j+1)\Gamma(n+\mu)\Gamma(K-\nu+1)\Gamma(\nu-j)}\, \xi^{\nu-K-j-1}. \tag{38}$$

4.1.2 Special case: SMI with infinite sample size

In case of infinite sample size, (33) can be expressed as

$$\begin{aligned} P_{\mathrm{d}}(\eta) &:= \lim_{K\to\infty} P_{\mathrm{d}}(\eta, K) \\ &= \sum_{\mu=0}^{\infty} \alpha_\mu \lim_{K\to\infty} \frac{\Gamma(K+1)\Gamma(K-\nu+\mu+1)}{\Gamma(K+\mu+1)\Gamma(K-\nu+1)} {}_1\mathrm{F}_1\left(K-\nu+\mu+1, K+\mu+1; -\bar{\xi}\right), \end{aligned} \tag{39}$$

where α_μ comprises all terms independent of K. Since $\Gamma(K+1) = K(K-1)\dots(K-\nu+1)\Gamma(K-\nu+1) = \left(K^\nu + \mathcal{O}(K^{\nu-1})\right)\Gamma(K-\nu+1)$ and similarly $\Gamma(K+\mu+1) = \left(K^\nu + \mathcal{O}(K^{\nu-1})\right)\Gamma(K+\mu+1-\nu)$, the limit inside the sum becomes

$$\begin{aligned}\lim_{K\to\infty} \frac{K^\nu + \mathcal{O}(K^{\nu-1})}{K^\nu + \mathcal{O}(K^{\nu-1})}\ {}_1\mathrm{F}_1\left(K-\nu+\mu+1, K+\mu+1; -\bar{\xi}\right) = \\ \lim_{K\to\infty} e^{-\bar{\xi}}{}_1\mathrm{F}_1\left(\nu, K+\mu+1; \bar{\xi}\right) = e^{-\bar{\xi}},\end{aligned} \tag{40}$$

such that

$$P_\mathrm{d}(\eta) = e^{-\xi}\sum_{\mu=0}^{\infty}\frac{\Gamma(n+\mu, n\eta)}{\Gamma(\mu+1)\Gamma(n+\mu)}\,\xi^\mu, \tag{41}$$

It is interesting to note that (41) is independent of ν and therewith of the number of channels N. In other words, if the covariance matrix is known one does not need to deploy a large array with many elements; $N = 2$ would already be sufficient to achieve the same P_d. Note, (41) has been derived independently as result (32) in [1]. However, for finite K and especially small training sets, the probability of detection depends on N according to (33) or (38).

4.1.3 Special case: SMI with $N = 2$ ($\nu = 1$)

For a two-channel system such as RADARSAT-2 or XWEAR applying SMI, i.e. $\nu = 1$, (33) becomes

$$P_\mathrm{d}(\eta) = \sum_{\mu=0}^{\infty}\frac{\Gamma(K+1)\Gamma(n+\mu, n\eta)B(K+\mu, 1)}{\Gamma(\mu+1)\Gamma(n+\mu)\Gamma(N-1)\Gamma(K)}\,\xi^\mu\,{}_1\mathrm{F}_1\left(K+\mu, K+\mu+1; -\xi\right). \tag{42}$$

Using the identities $B(K+\mu, 1) = 1/(K+\mu)$ and ${}_1\mathrm{F}_1\left(K+\mu, K+\mu+1; -\xi\right) = \frac{K+\mu}{\xi^{K+\mu}}\gamma(K+\mu, \xi)$ as well asUsing $\Gamma(K+1) = K\Gamma(K)$, we get

$$P_\mathrm{d}(\eta, K) = \sum_{\mu=0}^{\infty}\frac{\Gamma(n+\mu, n\eta)}{\Gamma(\mu+1)\Gamma(n+\mu)}\,\frac{K}{\xi^K}\,\gamma(K+\mu, \xi). \tag{43}$$

Alternatively one can set $j = 0$ and $\nu = 1$ in (38) to get (43).

4.2 Random target signal

4.2.1 General number of channels

By adopting the generic Gamma distribution for A in [1] with pdf

$$f_A(a) = \frac{1}{\Gamma(s)\bar{\xi}^s}\,a^{s-1}\,\exp\left\{-\frac{a}{\bar{\xi}}\right\}, \tag{44}$$

Table 2: *Relationship between Target Models and parameter s*

Parameter s	Target Model
$0 < s < 1$	Weinstock [26]
$s = 1$	Swerling I
$s = L$	Swerling II
$s = 2$	Swerling III
$s = 2L$	Swerling IV
$s \to \infty$	constant RCS

where

$$\bar{\xi} = \frac{\xi}{s} = \frac{L}{s}\sigma_t^2 \, \boldsymbol{d}^* \mathbf{R}^{-1} \boldsymbol{d}. \tag{45}$$

Various models may be expressed through the sole shape parameter s: The less used Swerling models III and IV are minor variants of the first two models with Γ_4 and Γ_{4L} distributions [31], respectively. Note, in all cases the expectation of A is approximately the SNR:

$$\begin{aligned} \mathsf{E}\, A \equiv \xi &= L\, \sigma_t^2 \, \boldsymbol{d}^* \mathbf{R}^{-1} \boldsymbol{d} \\ &\cong L \frac{\sigma_t^2}{\sigma_n^2} N \qquad \text{if} \qquad \sigma_c^2 >> \sigma_n^2, \ \|\boldsymbol{d}\|^2 = N. \end{aligned} \tag{46}$$

Now, the marginal test pdf can be expressed as the double integral

$$f_T(t) = \int_0^1 \int_0^\infty f_{(T|A,K)}(t; a, \kappa)\, f_A(a)\, f_K(\kappa)\, da\, d\kappa.$$

Using (44) and by integrating over t, see (34), the detection probability reads

$$\begin{aligned} P_{\mathrm{d}}(\eta, K, s) = \sum_{\mu=0}^{\infty} & \frac{\Gamma(n+\mu, n\eta)\Gamma(K+1)\bar{\xi}^{-s}}{\Gamma(\mu+1)\Gamma(n+\mu)\Gamma(\nu)\Gamma(K-\nu+1)\Gamma(s)} \\ & \times \int_0^\infty a^{s+\mu-1} e^{-\frac{1}{\bar{\xi}}a} \underbrace{\int_0^1 \kappa^{K-\nu+\mu}(1-\kappa)^{\nu-1} e^{-\kappa a}\, d\kappa}_{B(\nu, K-\nu+\mu+1)\, {}_1\mathrm{F}_1(K-\nu+\mu+1, K+\mu+1; -a)} \quad da, \end{aligned} \tag{47}$$

where we for the inner integral have used the result in [30][p.343-3.833-1]. Using the identity ${}_1\mathrm{F}_1\left(a, b; -x\right) = e^{-x} {}_1\mathrm{F}_1\left(b-a, b; x\right)$ is leading to

$${}_1\mathrm{F}_1\left(K-\nu+\mu+1, K+\mu+1; -a\right) = e^{-a} {}_1\mathrm{F}_1\left(\nu, K+\mu+1; a\right)$$

and with $B(\nu, K-\nu+\mu+1) = \Gamma(\nu)\Gamma(K+\mu-\nu+1)/\Gamma(K+\mu+1)$ we yield

$$P_{\mathrm{d}}(\eta, K, s) = \sum_{\mu=0}^{\infty} \frac{\Gamma(n+\mu, n\eta)\Gamma(K+1)\Gamma(K-\nu+\mu+1)\bar{\xi}^{-s}}{\Gamma(\mu+1)\Gamma(n+\mu)\Gamma(K-\nu+1)\Gamma(s)\Gamma(K+\mu+1)} \times \underbrace{\int_0^{\infty} a^{s+\mu-1} e^{-\left(1+\frac{1}{\xi}\right)a} {}_1\mathrm{F}_1\left(\nu, K+\mu+1; a\right)\, da}_{\Gamma(s+\mu)\left(1+\frac{1}{\xi}\right)^{-(s+\mu)} {}_2\mathrm{F}_1\left(\nu, s+\mu; K+\mu+1; \frac{\bar{\xi}}{1+\xi}\right)}, \tag{48}$$

where we used the result in [30][p.816-4]. This finally results in

$$\boxed{P_{\mathrm{d}}(\eta, K, s) = \sum_{\mu=0}^{\infty} \frac{\Gamma(n+\mu, n\eta)}{\Gamma(n+\mu)} \frac{\Gamma(K+1)\Gamma(K-\nu+\mu+1)\Gamma(s+\mu)}{\Gamma(\mu+1)\Gamma(K-\nu+1)\Gamma(s)\Gamma(K+\mu+1)} \times \frac{\bar{\xi}^{\mu}}{(1+\bar{\xi})^{s+\mu}} {}_2\mathrm{F}_1\left(\nu, s+\mu; K+\mu+1; \frac{\bar{\xi}}{1+\bar{\xi}}\right).} \tag{49}$$

In many cases the evaluation of the Gauss hypergeometric function is numerically challenging. In order to get a more numerical stable expression for (49), we can use the identity

$${}_2\mathrm{F}_1\left(\nu, s+\mu; K+\mu+1; \frac{\bar{\xi}}{1+\bar{\xi}}\right) = (1+\bar{\xi})^{s+\mu} {}_2\mathrm{F}_1\left(s+\mu, K+\mu+1-\nu; K+\mu+1; -\bar{\xi}\right). \tag{50}$$

Using the integral representation of the hypergeometric function in (50), see [32]:

$${}_2\mathrm{F}_1\left(s+\mu, K+\mu+1-\nu; K+\mu+1; -\bar{\xi}\right) = \frac{\Gamma(K+\mu+1)}{\Gamma(K+\mu+1-\nu)\Gamma(\nu)} \int_0^1 \frac{\kappa^{K-\nu+\mu}(1-\kappa)^{\nu-1}}{(1+\bar{\xi}\kappa)^{s+\mu}}\, d\kappa, \tag{51}$$

the detection probability can be evaluated through

$$P_{\mathrm{d}}(\eta, K, s) = \sum_{\mu=0}^{\infty} \frac{\Gamma(K+1)\Gamma(s+\mu)\Gamma(n+\mu, n\eta)}{\Gamma(\mu+1)\Gamma(n+\mu)\Gamma(\nu)\Gamma(K-\nu+1)\Gamma(s)} \bar{\xi}^{\mu} \int_0^1 \frac{\kappa^{K-\nu+\mu}(1-\kappa)^{\nu-1}}{(1+\bar{\xi}\kappa)^{s+\mu}}\, d\kappa. \tag{52}$$

For large SNR, $\bar{\xi}$, it is more efficient to re-write (52) so that the integral behaves

numerically more favorable even for increasing indices μ:

$$P_{\mathrm{d}}(\eta, K, s) = \sum_{\mu=0}^{\infty} \frac{\Gamma(n+\mu, n\eta)}{\Gamma(n+\mu)} \frac{\Gamma(K+1)\Gamma(s+\mu)}{\Gamma(\mu+1)\Gamma(\nu)\Gamma(K-\nu+1)\Gamma(s)} \times \left(\frac{1}{\bar{\xi}}\right)^{s} \int_0^1 \frac{\kappa^{K-\nu-s}(1-\kappa)^{\nu-1}}{\left(1+\frac{1}{\bar{\xi}\kappa}\right)^{s+\mu}} d\kappa. \tag{53}$$

4.2.2 Special case: SMI with infinite sample size

In case of infinite sample size, (49) can be expressed as

$$\begin{aligned} P_{\mathrm{d}}(\eta, s) &:= \lim_{K\to\infty} P_{\mathrm{d}}(\eta, K, s) \\ &= \sum_{\mu=0}^{\infty} \alpha_\mu \lim_{K\to\infty} \frac{\Gamma(K+1)\Gamma(K-\nu+\mu+1)}{\Gamma(K+\mu+1)\Gamma(K-\nu+1)} {}_2\mathrm{F}_1\left(\nu, s+\mu; K+\mu+1; \frac{\bar{\xi}}{1+\bar{\xi}}\right), \end{aligned} \tag{54}$$

where α_μ comprises all terms independent of K. Since $\Gamma(K+1) = K(K-1)\dots(K-\nu+1)\Gamma(K-\nu+1) = \left(K^\nu + \mathcal{O}(K^{\nu-1})\right)\Gamma(K-\nu+1)$ and similarly $\Gamma(K+\mu+1) = \left(K^\nu + \mathcal{O}(K^{\nu-1})\right)\Gamma(K+\mu+1-\nu)$, the limit inside the sum becomes

$$\lim_{K\to\infty} \frac{K^\nu + \mathcal{O}(K^{\nu-1})}{K^\nu + \mathcal{O}(K^{\nu-1})} \; {}_2\mathrm{F}_1\left(\nu, s+\mu; K+\mu+1; \frac{\bar{\xi}}{1+\bar{\xi}}\right) = 1, \tag{55}$$

such that

$$P_{\mathrm{d}}(\eta, s) = \sum_{\mu=0}^{\infty} \frac{\Gamma(n+\mu, n\eta)}{\Gamma(n+\mu)} \frac{\Gamma(s+\mu)}{\Gamma(s)\Gamma(\mu+1)} \frac{\bar{\xi}^\mu}{(1+\bar{\xi})^{s+\mu}}. \tag{56}$$

Again, as in the deterministic target scenario, the $P_{\mathrm{d}}(\eta, s)$ (56) is also independent of ν and therewith of the number of channels[3] N. In other words, if the covariance matrix is known a small N would already be sufficient to achieve identical P_{d}. Note, (56) has been derived independently in [1]. For instance, it is identical to equation (49) in [1] for homogeneous clutter, i.e. $\Delta = \delta = 1$ so that the SCNR(1) in equation (48) of [1] equals $\bar{\xi}$ in (56) above. However, for finite K, and especially small training sets, the probability of detection depends on N according to (53).

[3]Except for the increase in SNR due to the higher antenna gain (larger N in (46)).

4.2.3 Special case: Infinite target model parameter

In Annex A it is shown that the detection probability for the deterministic target model, i.e. a constant RCS, can be derived as the limiting case of (49) for $s \to \infty$:

$$\begin{aligned} P_{\mathrm{d}}(\eta, K; \xi) &:= \lim_{s\to\infty} P_{\mathrm{d}}(\eta, K, s; \tfrac{\xi}{s}) \\ &= \sum_{\mu=0}^{\infty} \frac{\Gamma(n+\mu, n\eta)}{\Gamma(n+\mu)} \frac{\Gamma(K+1)\Gamma(K-\nu+\mu+1)}{\Gamma(\mu+1)\Gamma(K-\nu+1)\Gamma(K+\mu+1)} \\ &\qquad \times \xi^{\mu}\ {}_1\mathrm{F}_1\left(K+\mu-\nu+1, K+\mu+1; -\xi\right), \end{aligned} \tag{57}$$

which is identical to (33). This transition is also demonstrated numerically in Fig. 3.

5 Numerical examples

This chapter presents several examples of the numerically evaluated ROC's for different filter estimation techniques, target signal models and varying parameter settings.

The required asymptotic covariance matrix has been computed to

$$\mathbf{R} = \sigma_c^2 \sum_{m=1}^{M} \boldsymbol{d}(u_m)\boldsymbol{d}(u_m)^* + \sigma_n^2 \mathbf{I}_N, \tag{58}$$

where σ_c^2 denotes the interference power level and σ_n^2 the noise power level, respectively, so that the interference-to-noise ration (INR) at a single antenna channel is $\mathrm{INR} = \sigma_c^2/\sigma_n^2$. Without loss of generality, the steering or Direction-of-Arrival vector $\boldsymbol{d} \in \mathbb{C}^{N\times 1}$ is given as a pure phase vector:

$$\boldsymbol{d}(u) = \left[1, e^{-j\frac{2\pi}{\lambda}d\,u}, \ldots, e^{-j\frac{2\pi}{\lambda}d(N-1)\,u}\right]'. \tag{59}$$

An X-band system with wavelength $\lambda = 3$ cm is chosen, and the antenna element distance d is $d = \lambda/2$ avoiding any grating lobes. The interference dimension was set to $M = 3$ with the corresponding directions $u_m = -[0.5, 0.2, 0.1]$. According to (19) the target signal was computed to $\boldsymbol{s}(u_t) = \sigma_t \boldsymbol{d}(u_t)$ while the target direction is $u_t = 0.5$ hence representing a sidelobe interference scenario with a given SNIR$=L \cdot$ SNR $\cdot\, \boldsymbol{d}(u_t)^* \mathbf{R} \boldsymbol{d}(u_t)$ with $\mathrm{SNR} = \sigma_t^2/\sigma_n^2$.

The false alarm rate P_{fa} was varied between 1 and 10^{-6} for all computations. The detection threshold η for a homogeneous Gaussian interference model given in (27) can in MATLAB conveniently determined using the single command:

$$\eta = \mathrm{gammaincinv}(P_{\mathrm{fa}}, n, '\mathrm{upper}')/n, \tag{60}$$

where the division by the number of looks stems from the scaling of the threshold n in (27).

For the smallest possible multi-channel system, a two-channel radar such as RADAR SAT-2 or XWEAR [33], using a constant target signal model and employing SMI, Figure Fig. 1 illustrates the improving performance when the sample size increases from $K = 2$ to infinity. For smaller training sample sizes there is a steady increase in performance while for values larger than $K = 50$, the curves are almost indistinguishable. For the black curve representing $K \to \infty$ we used (41).

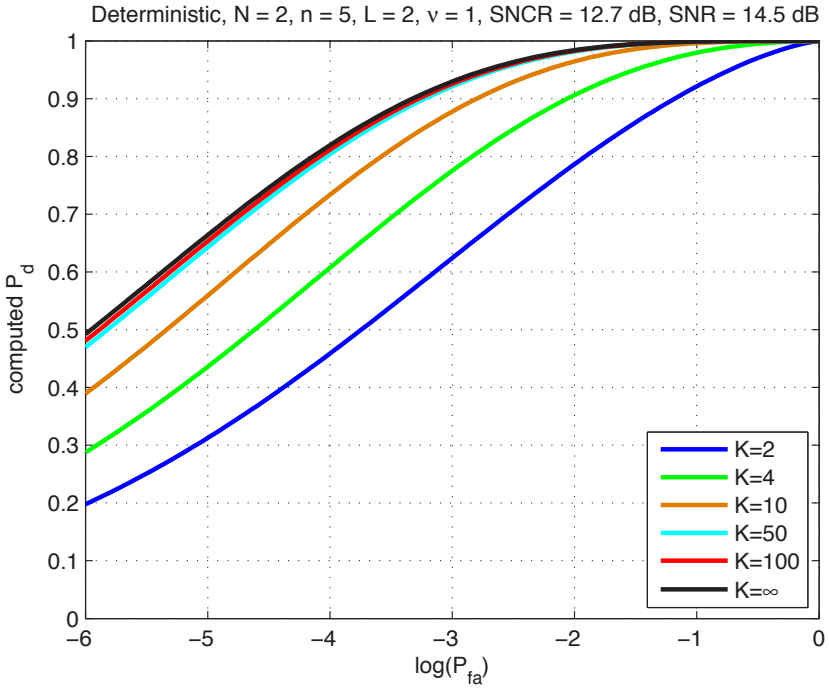

Figure 1: *ROCs of SMI for varying number of training samples for a small array.*

Fig. 2 shows essentially the same scenario but for a somewhat larger array with $N = 10$ channels. Again, the performance is steadily improving until about $K \cong 20{\cdot}N$ at which it gets close to the optimum curve. This figure is a good example to highlight that the SNIR loss factor is not sufficient to judge full capabilities. According to (14) the average number of training data to achieve a 3 dB loss in SNIR is about $K = 20$, which however may clearly not sufficient in terms of P_{d} especially for smaller P_{fa}.

Fig. 3 illustrates two facts. First, the drastically reduced P_{d} when a Swerling I target model is used compared to the determinsitic model in Fig. 2. Second, it demonstrates how the P_{d} for a Swerling target in (49) converges toward the one for deterministic targets in (33) (black curve) if s tends to infinity.

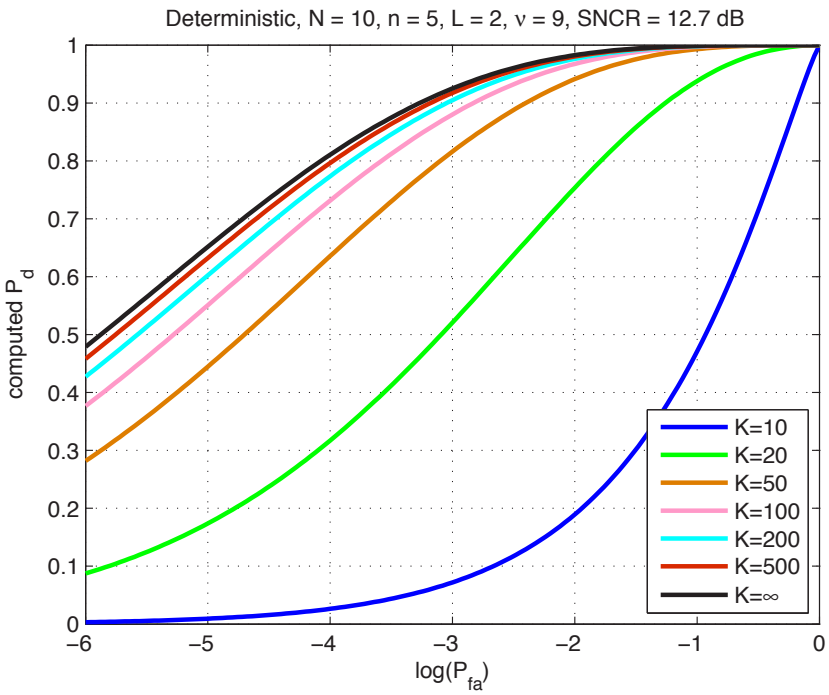

Figure 2: *ROCs of SMI for varying number of training samples for a larger array.*

Fig. 4 illustrates the change in detectability of a deterministic target as a function of the number of sensor elements, given a fixed number of training samples $K = 20$. One can recognize that the P_d raises sharply from $N = 2$ to $N = 8$, then stays quasi constant for $N = 12$, and then drops back rapidly until $N = 20$. At first glance this seems counterintuitive since the SNR increases steadily for larger N; Nevertheless for larger arrays the training sample size is too small and hence the uncertainty in the estimation of the covariance matrix severely starts to limit the performance.

Fig. 5 demonstrates how the provided equations permit comparison of different filter estimation techniques exemplified with SMI and Loaded SMI, see Table 1. On one hand, it is interesting to note that LSMI is better than SMI over the entire false alarm range. On the other hand, comparing the ROCs of one technique but for different target models reveals an intersection point after which the random model shows higher detectability than the constant target signal model.

Fig. 6 illustrates the improvement of detection performance invoked by increasing SNR for a given array size and training sample size, respectively. The LSMI method was chosen. Once can see that the increase in detection probability does not follow linearly the increase in SNIR, hence again demonstrating that the simple SNIR loss factor does not provide the full picture.

Fig. 7 and Fig. 8 depict the detectability loss against the optimum P_d (with exactly

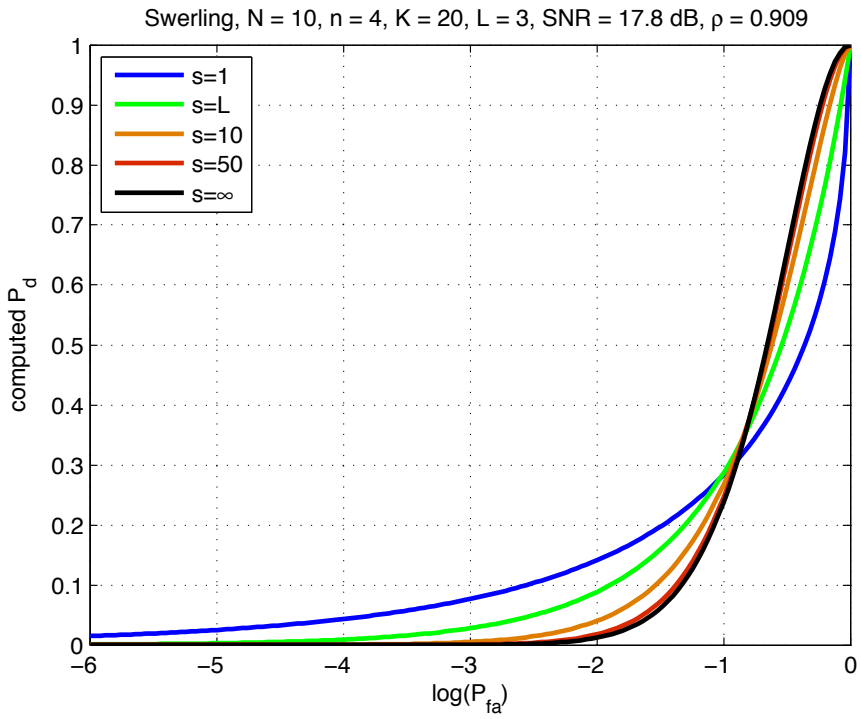

Figure 3: *ROCs of SMI for Swerling target for an increasing target model parameter s. The black curve has been computed using* (33).

known covariance matrix) for varying number of training samples used to estimate the covariance number for a deterministic and fluctuating target model, respectively. For a given operating point, i.e. P_{fa}, these curves will tell a radar designer what the minimum number K shall be, in order to achieve a given percentage of the optimum detectability. For instance, if one wishes to achieve at least 50% detection probability for a given false alarm rate of 10^{-6}, then for a deterministic target ones needs to provide about 40 training samples, and for a Swerling I target about 10 to 15 less.

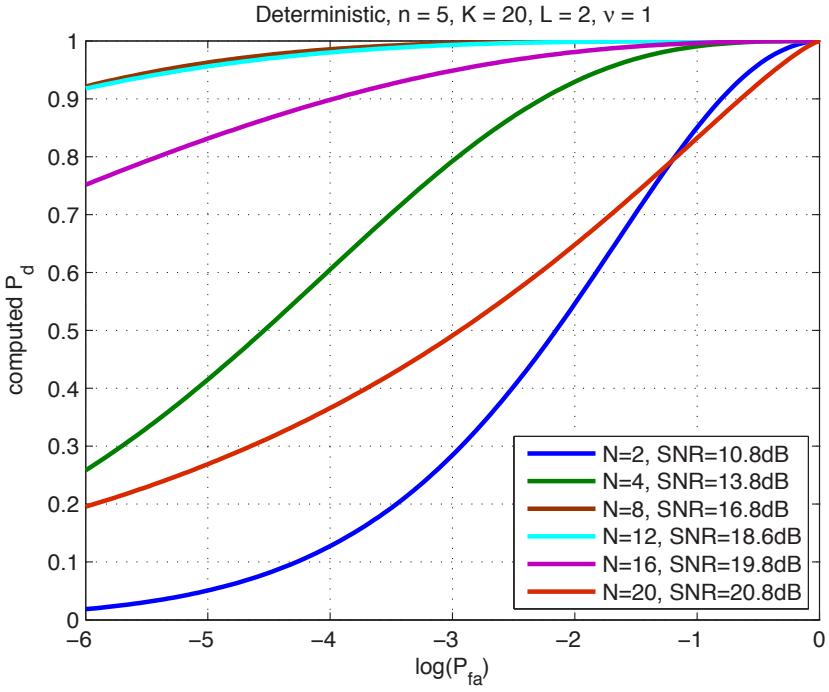

Figure 4: *ROCs of SMI for a deterministic target and varying number of elements.*

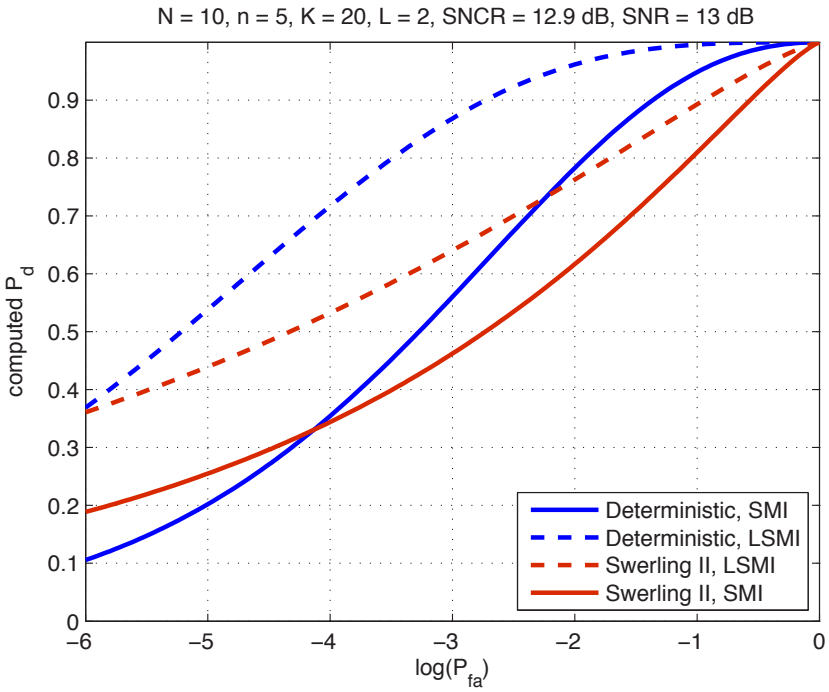

Figure 5: *ROC of SMI and LSMI for constant target and Swerling II model.*

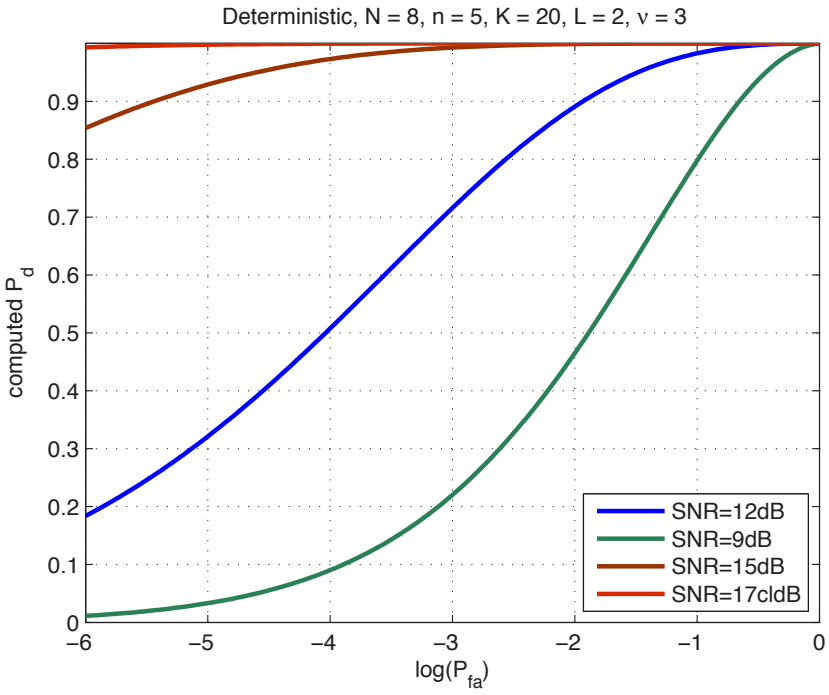

Figure 6: *ROC of LSMI for increasing SNR.*

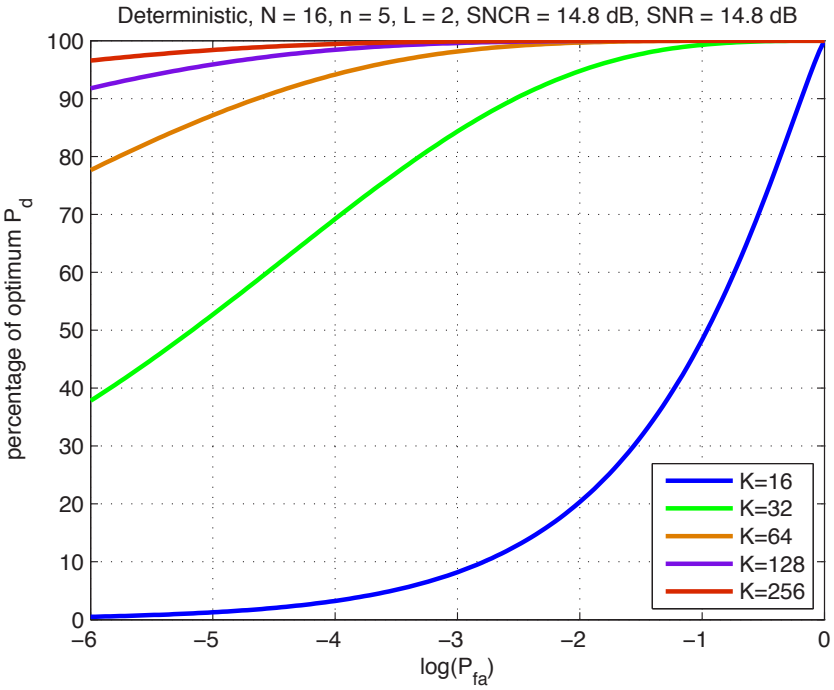

Figure 7: *Deviation of the P_{d} of SMI from the optimum value for increasing number of training samples K; Deterministic target model.*

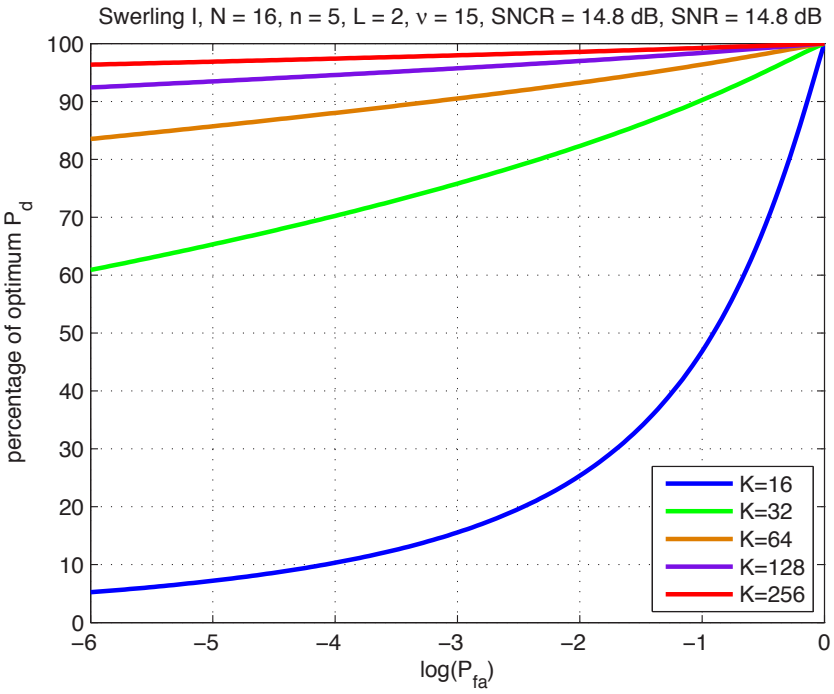

Figure 8: *Deviation of the P_{d} of SMI from the optimum value for increasing number of training samples K; Swerling I target model.*

6 Summary and conclusions

This memorandum presented several novel closed-form mathematical expressions to compute the Receiver Operating Characteristics of multi-channel adaptive detectors, used in applications such as STAP for GMTI or interference suppression via adaptive beamforming in phased array antennas under the assumption of an homogeneous interference environment. As a novelty, the presented performance analysis and numerical approaches comprise all practically relevant techniques to estimate the adapted filter vector based on a set of independent secondary training data. The presented work can be seen an extension or generalization of previous work, [1], in which the covariance matrix and hence the filter vector was presumed to be known.

The dimensionality of the array, the primary and secondary data sets, the interference rank as well as power levels are freely selectable and together with interchangeable target signal statistics (all Swerling cases including deterministic) offer a sufficient breadth to cover a wide range of scenarios. It was found that all of these parameters have a distinct impact on the achievable ROC in contrast to results in previous publications which indicated dependency mainly on the number of channels. The utility and usefulness of the theoretical work has been demonstrated with examples featuring a variety of different parameter settings and estimation methods. The presented numerical recipes have been proven to be efficient and robust. They are capable of numerically handling arrays consisting of several hundreds receiver channels using several hundreds training samples effortlessly. The computation time on a conventional desktop computer is in the order of seconds. Note that a purely simulation-based approach is unfeasible for large sized arrays.

Although the provided theoretical analysis has been limited to non-classical detector schemes due to mathematical tractability, it is a very important step towards a complete unifying theoretical framework that will eventually include most practical detectors, all relevant adaptive weight estimators and even impact of target signal mismatches. Another important and non-trivial open topic for future work would be to extend the provided theoretical derivation to heterogeneous interference environments. Heterogeneity is commonly modeled through use of an additional independent texture random variable applied to the clutter, see for instance [1]. Including this so-called compound model, unfortunately, does not permit to write the pdf of the test statistic (21) as a function of the SNIR loss factor κ anymore. As this was the prerequisite for the proposed analysis, heterogeneity makes the mathematical derivation much more challenging. Perhaps the results and techniques may be useful for tackling the heterogeneous case.

References

[1] Gierull, C. H. (2011), Numerical Recipes to Determine the Performance of Multi-Channel GMTI Radars, (Technical Memorandum TM 2011-230) DRDC Ottawa.

[2] Kelly, E. (1989), Performance of an adaptive detection algorithm; rejection of unwanted signals, *Aerospace and Electronic Systems, IEEE Transactions on*, 25(2), 122–133.

[3] Richmond, C. D. (2000), Performance of the adaptive sidelobe blanker detection algorithm in homogeneous environments, *Signal Processing, IEEE Transactions on*, 48(5), 1235–1247.

[4] Nickel, U. (2006), Principles of Adaptive Array Processing, (Educational Notes RTO-EN-SET-086) NATO RTO, Neuilly-sur-Seine, France.

[5] Boroson, D. M. (1980), Sample size considerations for adaptive arrays, *Aerospace and Electronic Systems, IEEE Transactions on*, 16(4), 446–451.

[6] Melvin, W. L. (2004), A STAP overview, *Aerospace and Electronic Systems Magazine, IEEE*, 19(1), 19–35.

[7] Cerutti-Maori, D., Sikaneta, I., and Gierull, C. H. (2012), Optimum SAR/GMTI processing and its application to the radar satellite RADARSAT-2 for traffic monitoring, *IEEE Trans. Geoscience and Remote Sensing*, 50(10), 3868–3881.

[8] Marcum, J. (1960), A statistical theory of target detection by pulsed radar, *Information Theory, IRE Transactions on*, 6(2), 59–267.

[9] Gierull, C. H. and Livingstone, C. (2004), SAR-GMTI Concept for RADARSAT-2, In Klemm, R., (Ed.), *The Applications of Space-Time Processing*, Stevenage, UK: IEE Press.

[10] Reed, L., Mallett, J. D., and Brennan, L. E. (1974), Rapid Convergence Rate in Adaptive Arrays, *IEEE Trans. Aerosp. and Electron. Systems*, AES-10(6), 853–863.

[11] Klemm, R. (1998), Space-Time Adaptive Processing, Stevenage, UK: IEE Press.

[12] Nitzberg, R. (1984), Detection loss of the sample matrix inversion technique, *Aerospace and Electronic Systems, IEEE Transactions on*, 20(6), 824–827.

[13] Wang, H. and Cai, L. (1990), On adaptive multiband signal detection with the SMI algorithm, *Aerospace and Electronic Systems, IEEE Transactions on*, 26(5), 768–773.

[14] Cai, L. and Wang, H. (1991), Performance comparisons of modified SMI and GLR algorithms, *Aerospace and Electronic Systems, IEEE Transactions on*, 27(3), 487–491.

[15] Carlson, B. D. (1988), Covariance Matrix Estimation Errors and Diagonal Loading in Adaptive Arrays, *IEEE Trans. Aerosp. and Electron. Systems*, AES-24(4), 397–401.

[16] Gierull, C. H. (1995), Schnelle Signalraumschätzung in Radaranwendungen (Fast Subspace Estimation for Radar Applications), Aachen, Germany: Shaker Verlag. Ph.D. Dissertation (in German), Ruhr-University Bochum.

[17] Cheremisin, O. P. (1982), Efficiency of Adaptive Algorithms With Regulized Sample Covariance Matrix (in Russian), *Radiotechnology and Electronics (Russia)*, 2(10), 1933–1941.

[18] Gierull, C. H. (1997), Statistical Analysis of the Eigenvector Projection Method for Adaptive Spatial Filtering of Interference, *IEE Proc. Radar, Sonar and Navig.*, 144(2), 57–63.

[19] Hung, E. K. and Turner, R. M. (1983), A Fast Beamforming Algorithm for Large Arrays, *IEEE Trans. Aerosp. and Electron. Systems*, AES-19(4), 589–607.

[20] Gierull, C. H. (1996), Performance Analysis of Fast Projections of the Hung-Turner Type for Adaptive Beamforming, *Signal Processing*, 50(1-2), 17–29.

[21] Gierull, C. H. (1997), A Fast Subspace Estimation Method for Adaptive Beamforming Based on Covariance Matrix Transformation, *AEÜ Int. J. Electr. Commun.*, 51(4), 187–232.

[22] Nickel, U. (1997), On the Application of Subspace Methods for Small Sample Size, *AEÜ Int. J. Electron. Commun.*, 51(6), 279–289.

[23] Gierull, C. H. and Balaji, B. (2002), Minimal sample support space-time adaptive processing with fast subspace techniques, *IEE Proc. Radar, Sonar and Navig.*, 149(5), 209–220.

[24] Nathanson, F. E. (1969), Radar Design Principles: Signal Processing and the Environment, McGraw-Hill.

[25] Mitchell, R. and Walker, J. (1971), Recursive methods for computing detection probabilities, *Aerospace and Electronic Systems, IEEE Transactions on*, 7(4), 671–676.

[26] Shnidman, D. (1976), Efficient evaluation of probabilities of detection and the generalized Q-function (Corresp.), *Information Theory, IEEE Transactions on*, 22(6), 746–751.

[27] Shnidman, D. A. (1995), Radar detection probabilities and their calculation, *IEEE Transactions on Aerospace and Electronic Systems*, 31(3), 928–950.

[28] Kelly, E. J. (1986), An adaptive detection algorithm, *Aerospace and Electronic Systems, IEEE Transactions on*, 28(2), 115–127.

[29] Robey, F. C., Fuhrmann, D. R., Kelly, E. J., and Nitzberg, R. (1992), A CFAR adaptive matched filter detector, *Aerospace and Electronic Systems, IEEE Transactions on*, 28(1), 208–216.

[30] Gradshteyn, I. S. and Ryzhik, I. M. (2000), Table of Integrals, Series and Products (Sixth Edition), 6 ed, Academic Press.

[31] Swerling, P. (1997), Radar probability of detection for some additional fluctuating target cases, *IEEE Transactions on Aerospace and Electronic Systems*, 33(2), 698–709.

[32] Abramowitz, M. and Stegun, I. A. (1970), Handbook of Mathematical Functions, 9 ed, Dover Publications, Inc.

[33] Damini, A., Haslam, G., Balaji, B., and Goulding, M. (2004), A new X-band Experimental Airborne Radar for SAR and GMTI, In *Proc. of EUSAR*, pp. 639–642, Ulm, Germany.

Annex A: Limit of $P_{\mathrm{d}}\,(49)$ for infinite target model parameter s

Using identity (50), the P_{d} for fluctuating target RCS in (49) reads:

$$P_{\mathrm{d}}(\eta, K, s) = \sum_{\mu=0}^{\infty} \frac{\Gamma(n+\mu, n\eta)}{\Gamma(n+\mu)} \frac{\Gamma(K+1)\Gamma(K-\nu+\mu+1)\Gamma(s+\mu)}{\Gamma(\mu+1)\Gamma(K-\nu+1)\Gamma(s)\Gamma(K+\mu+1)} \times \bar{\xi}^{\mu}\ {}_2\mathrm{F}_1\left(s+\mu, K+\mu-\nu+1; K+\mu+1; -\bar{\xi}\right). \tag{A.1}$$

According to Table 2 in section 4.2.1, the limit $s \to \infty$ corresponds to the deterministic target model, sometimes also called Swerling 0. Considering only the terms depending on s in (A.1) and remembering that $\bar{\xi} = \frac{\xi}{s}$, the task at hand is to evaluate the following limit:

$$\lim_{s\to\infty} F(s) = \lim_{s\to\infty} \frac{\Gamma(s+\mu)}{\Gamma(s)} \frac{1}{s^{\mu}}\ {}_2\mathrm{F}_1\left(s+\mu, K+\mu-\nu+1; K+\mu+1; -\tfrac{\xi}{s}\right). \tag{A.2}$$

Using the general series definition of the hypergeometric function, e.g. [32], the limit can be re-written as

$$\begin{aligned}\lim_{s\to\infty} F(s) &= \lim_{s\to\infty} \frac{\cancel{\Gamma(s+\mu)}}{\Gamma(s)s^{\mu}} \frac{\Gamma(K+\mu+1)}{\cancel{\Gamma(s+\mu)}\Gamma(K+\mu-\nu+1)} \\ &\quad \times \sum_{m=0}^{\infty} \frac{\Gamma(s+\mu+m)\Gamma(K+\mu-\nu+1+m)}{\Gamma(K+\mu+1+m)} \frac{(-\xi)^m}{m!s^m} \\ &= \sum_{m=0}^{\infty} \frac{\frac{\Gamma(K+\mu-\nu+1+m)}{\Gamma(K+\mu-\nu+1)}}{\frac{\Gamma(K+\mu+1+m)}{\Gamma(K+\mu+1)}} \frac{(-\xi)^m}{m!} \lim_{s\to\infty} \frac{\Gamma(s+\mu+m)}{\Gamma(s)\, s^{m+\mu}}.\end{aligned} \tag{A.3}$$

Using the identity

$$\begin{aligned}\Gamma(s+\mu+m) &= (s+\mu+m-1)\cdot(s+\mu+m-2)\cdots(s+1)\cdot s\,\Gamma(s) \\ &= \left[s^{\mu+m} + \mathcal{O}\left(s^{m+\mu-1}\right)\right]\Gamma(s)\end{aligned}$$

one can see that the limit in (A.3) tends towards one for any μ, so that

$$\lim_{s\to\infty} F(s) = \sum_{m=0}^{\infty} \frac{(K+\mu-\nu+1)_m}{(K+\mu+1)_m} \frac{(-\xi)^m}{m!} = {}_1\mathrm{F}_1\left(K+\mu-\nu+1, K+\mu+1; -\xi\right), \tag{A.4}$$

where $(a)_m = \frac{\Gamma(a+m)}{\Gamma(a)}$ denotes the Pochhammer symbol, [32]. Inserting (A.4) into (A.1) confirms the correctness of (33), which was alternatively derived based on the deterministic target model in section 4.1.1.

This page intentionally left blank.

Annex B: Derivation of the pdf of the SNIR loss factor for the HTP

As shown in [20], for the HTP the pdf of the SNIR loss factor $\mathcal{K}_l$ in (24) is given as the product of two independent beta-distributed random variables with $2(N-K), 2(K-M)$, and $2(K-M+1), 2M$ degrees of freedoms respectively. The filter vector is being created as

$$\hat{\boldsymbol{U}} = \left(\mathbf{I} - \mathbf{X}\left(\mathbf{X}^{*}\mathbf{X}\right)^{-1}\mathbf{X}^{*}\right)\boldsymbol{d}, \tag{B.1}$$

with $\mathbf{X} = [\boldsymbol{X}_1, \ldots, \boldsymbol{X}_K]$ is a matrix whose columns are made up by the K secondary data vectors. Consequently, in comparison to the other estimation methods, for HTP the number of training samples is limited by $1 \leq K < N$.

In the following a new closed form expression for the product pdf will be derived that in turn leads to a closed form expression for the achievable probability of detection, see Annex C. Let $Z = Z_1 \cdot Z_2$ be the product of the two beta-distributed variables with pdfs according to (25):

$$f_{Z_1}(z_1) = \frac{1}{B(N-K, K-M)}\, z_1^{N-K-1}\,(1-z_1)^{K-M-1} \quad 0 < z_1 \leq 1 \tag{B.2}$$

$$f_{Z_2}(z_2) = \frac{1}{B(K-M+1, M)}\, z_2^{K-M}\,(1-z_2)^{M-1} \quad 0 < z_2 \leq 1, \tag{B.3}$$

for which the product pdf can be computed via

$$f_Z(z) = \int_{-\infty}^{\infty} \frac{1}{|w|}\, f_{Z_1}(w)\; f_{Z_2}\left(\tfrac{z}{w}\right)\; dw \tag{B.4}$$

with $z \leq w \leq 1$, leading to

$$f_Z(z) = \frac{B(K-M+1, M)^{-1}}{B(N-K, K-M)}\, z^{K-M} \int_{z}^{1} w^{N-2K-1}\,(1-w)^{M-1}\,(w-z)^{M-1}\; dw. \tag{B.5}$$

Applying the variable transformation $(w-z) \mapsto x$ and using the result [30] [p.315-8] yields

$$f_Z(z) = \tfrac{B(K-M,M)}{B(N-K,K-M)B(K-M+1,M)}\, z^{N-M-K-1}\,(1-z)^{K-1}\,{}_2\mathrm{F}_1\left(2K+1-N, M; K; \tfrac{z-1}{z}\right), \tag{B.6}$$

where ${}_2F_1(\cdot)$ denotes the hypergeometric function. Using $B(a,b) = \frac{\Gamma(a)\Gamma(b)}{\Gamma(a+b)}$ and the identity [30] [p.998-9.131.1]

$${}_2\mathrm{F}_1\left(2K+1-N, M; K; -\frac{1-z}{z}\right) = z^M\,{}_2\mathrm{F}_1\left(M, N-K-1; K; 1-z\right), \tag{B.7}$$

finally results in

$$f_Z(z) = \frac{K\,\Gamma(N-M)}{\Gamma(N-K)\Gamma(K-M+1)}\, z^{N-K-1}\,(1-z)^{K-1}\,{}_2\mathrm{F}_1\left(M, N-K-1; K; 1-z\right), \tag{B.8}$$

with $0 < z \leq 1$. A simple test that (B.8) is indeed a density function is achieved by integrating the three z-dependent terms after applying the transformation $(1-z) \mapsto x$, i.e.

$$\int_0^1 (1-x)^{N-K-1}\, x^{K-1}\,{}_2\mathrm{F}_1\left(M, N-K-1; K; x\right)\; dx, \tag{B.9}$$

which, using the result [30] [p.806-7.512.4] becomes

$$\frac{\cancel{\Gamma(K)}\Gamma(N-K)\Gamma(K-M+1)}{\Gamma(N-M)\cancel{\Gamma(K+1)}} \quad \cancel{K\Gamma(K)} \tag{B.10}$$

equaling the inverse of the constant in (B.8), and hence confirming $\int_0^1 f_Z(z)\,dz = 1$.

Annex C: Probability of detection of a deterministic target using HTP

Using (30) and (31) the P_{d} of any estimation technique, for which a density function $\mathcal{K}$ exists, can be computed via $\int_{\eta}^{\infty} f_T(t)\,dt$, i.e.

$$f_T(t) = \sum_{\mu=0}^{\infty} \frac{\Gamma(n+\mu, n\eta)}{\Gamma(n+\mu)} \frac{\xi^{\mu}}{\Gamma(\mu+1)} \int_0^1 e^{-\xi\kappa}\,\kappa^{\mu}\, f_{\mathcal{K}}(\kappa)\,d\kappa, \tag{C.1}$$

where it has been used that the integral with respect to t involves to the incomplete Gamma function, see (34). Utilizing the pdf for HTP in (B.8) and disregarding for a moment the constant terms, the following integral needs to be computed:

$$\int_0^1 \kappa^{N-K+\mu-1}\,(1-\kappa)^{K-1}\,\exp\left(-\xi\kappa\right)\,{}_2\mathrm{F}_1\left(M, N-K-1; K; 1-\kappa\right)\,d\kappa. \tag{C.2}$$

Applying the variable transformation $(1-\kappa) \mapsto x$ and using the result in [30] [p.809-7.523], the integral evolves to

$$e^{-\xi} \underbrace{\int_0^1 (1-x)^{N-K+\mu-1}\,x^{K-1}\,e^{\xi x}\,{}_2\mathrm{F}_1\left(M, N-K-1; K; x\right)\,dx}_{\frac{\Gamma(K)\Gamma(N-K+\mu)\Gamma(K-M+\mu+1)}{\Gamma(N-M+\mu)\Gamma(K+\mu+1)}\,e^{\xi}\,{}_2\mathrm{F}_2(K,K-M+\mu+1,N-M+\mu,K+\mu+1;-\xi)}, \tag{C.3}$$

where ${}_2\mathrm{F}_2(\cdot)$ denotes the generalized hypergeometric function. Considering the constant terms in (B.8) finally yields:

$$\begin{aligned} P_{\mathrm{d}}(\eta, K) = \sum_{\mu=0}^{\infty} & \frac{\Gamma(n+\mu, n\eta)}{\Gamma(n+\mu)} \frac{(N-K)_{\mu}(K-M+1)_{\mu}}{(N-M)_{\mu}(K+1)_{\mu}} \frac{\xi^{\mu}}{\Gamma(\mu+1)} \\ & \times\ {}_2\mathrm{F}_2\left(K, K-M+\mu+1, N-M+\mu, K+\mu+1; -\xi\right), \end{aligned} \tag{C.4}$$

where $(a)_m = \frac{\Gamma(a+m)}{\Gamma(a)}$ denotes the Pochhammer symbol, [32].

This page intentionally left blank.

Annex D: Performance analysis of Test b)

For the normalization of Test b) in (22) the pdf in (21) becomes

$$\begin{aligned} f_{T|A,\mathcal{K}}(t;a,\kappa) &= n\,|\boldsymbol{u}^*\boldsymbol{d}|^2 f_{\bar{T}|A,\mathcal{K}}(n\,|\boldsymbol{u}^*\boldsymbol{d}|^2\,\bar{t};a,\kappa,\sigma^2) \\ &= n\,|\boldsymbol{u}^*\boldsymbol{d}|^2 \left(\frac{1}{\boldsymbol{u}^*\mathbf{R}\boldsymbol{u}}\right)^{\frac{n+1}{2}} \left(\frac{n|\boldsymbol{u}^*\boldsymbol{d}|^2\,t}{a\kappa}\right)^{\frac{n-1}{2}} \\ &\quad \times \exp\left(-\frac{n\,|\boldsymbol{u}^*\boldsymbol{d}|^2}{\boldsymbol{u}^*\mathbf{R}\boldsymbol{u}}t - a\kappa\right)\ \mathrm{I}_{n-1}\left(2\sqrt{a\,\kappa\,\frac{n\,|\boldsymbol{u}^*\boldsymbol{d}|^2}{\boldsymbol{u}^*\mathbf{R}\boldsymbol{u}}\,t}\right). \end{aligned} \tag{D.1}$$

Exploiting that $\frac{\boldsymbol{d}^*\mathbf{R}^{-1}\boldsymbol{d}}{\boldsymbol{d}^*\mathbf{R}^{-1}\boldsymbol{d}}\,\frac{|\boldsymbol{u}^*\boldsymbol{d}|^2}{\boldsymbol{u}^*\mathbf{R}\boldsymbol{u}} = \boldsymbol{d}^*\mathbf{R}^{-1}\boldsymbol{d}\,\kappa$ at the appropriate places in (D.1) we get

$$\begin{aligned} f_{T|A,\mathcal{K}}(t;a,\kappa) &= \left(n\boldsymbol{d}^*\mathbf{R}^{-1}\boldsymbol{d}\right)^{\frac{n+1}{2}}\,\kappa^{\frac{n+1}{2}} \left(\frac{t}{a\kappa}\right)^{\frac{n-1}{2}} \\ &\quad \times \exp\left(-n\boldsymbol{d}^*\mathbf{R}^{-1}\boldsymbol{d}\,\kappa\,t - a\kappa\right)\ \mathrm{I}_{n-1}\left(2\kappa\sqrt{n\boldsymbol{d}^*\mathbf{R}^{-1}\boldsymbol{d}\,a\,t}\right). \end{aligned} \tag{D.2}$$

Using the variable transform $T' \mapsto Tn\boldsymbol{d}^*\mathbf{R}^{-1}\boldsymbol{d}$ where $t' \in \{0,\infty\}$, the pdf (D.2) simplifies to

$$f_{T'|A,\mathcal{K}}(t';a,\kappa) = \kappa\left(\frac{t'}{a}\right)^{\frac{n-1}{2}}\ \exp\left(-(t'+a)\kappa\right)\ \mathrm{I}_{n-1}\left(2\kappa\sqrt{a\,t'}\right), \tag{D.3}$$

which only depends on a and κ.

D.1 Probability of false alarm

In the absence of a target, i.e. $a = 0$, the conditional pdf (D.3) reads

$$f_{T|\mathcal{K}}(t;\kappa) = \frac{\kappa^n}{\Gamma(n)}t^{n-1}\ e^{-t\,\kappa}, \tag{D.4}$$

so that the P_{fa} corresponding to the threshold η results from the double integration:

$$\begin{aligned} P_{\mathrm{fa}}(\eta) &= \int_0^1 \frac{\cancel{\kappa^n}}{\Gamma(n)}\ f_{\mathcal{K}}(\kappa) \underbrace{\int_\eta^\infty t^{n-1}\,e^{-t\,\kappa}\,dt}_{\frac{\Gamma(n,\eta\,\kappa)}{\cancel{\kappa^n}}}\ d\kappa \\ &= \int_0^1 \frac{\Gamma(n,\eta\,\kappa)}{\Gamma(n)}\ f_{\mathcal{K}}(\kappa)\ d\kappa = \mathsf{E}_{\mathcal{K}}\,\frac{\Gamma(n,\eta\,\mathcal{K})}{\Gamma(n)}, \end{aligned} \tag{D.5}$$

which in contrast to (27) still depends on the SNIR loss κ. The incomplete gamma-function in (D.5) can be replaced by the finite sum expression

$$\Gamma(n,\eta\kappa) = \Gamma(n)e^{-\eta\kappa}\sum_{m=0}^{n-1}\frac{\eta^m\,\kappa^m}{\Gamma(m+1)} \tag{D.6}$$

and after some algebra and using the fact that

$$\int_0^1 \kappa^{K-\nu+m}\,(1-\kappa)^{\nu-1}\,e^{-\eta\kappa}\,d\kappa = B(\nu,K-\nu+m+1)\,e^{-\eta}\,{}_1\mathrm{F}_1\,(\nu,K+m+1;\eta) \tag{D.7}$$

we finally yield

$$P_{\mathrm{fa}}(\eta) = \sum_{m=0}^{n-1}\frac{\Gamma(K+1)\Gamma(K-\nu+m+1)}{\Gamma(K-\nu+1)\Gamma(m+1)\Gamma(K+m+1)}\,\eta^m\,e^{-\eta}\,{}_1\mathrm{F}_1\,(\nu,K+m+1;\eta)\,. \tag{D.8}$$

D.2 Probability of detection

Inserting the power series representation of the Bessel-function

$$\mathrm{I}_{n-1}\left(2\kappa\sqrt{a\,t}\right) = \sum_{\mu=0}^{\infty}\frac{\kappa^{n-1+2\mu}\,(at)^{\frac{n-1+2\mu}{2}}}{\Gamma(\mu+1)\Gamma(n+\mu)} \tag{D.9}$$

into (D.3) leads to

$$\begin{aligned} f_{T|A,\mathcal{K}}(t;a,\kappa) = \sum_{\mu=0}^{\infty}\underbrace{\frac{\Gamma(K+1)\Gamma(\mu+1)^{-1}\Gamma(n+\mu)^{-1}}{\Gamma(\nu)\Gamma(K-\nu+1)\Gamma(s)}\,\frac{1}{\bar{\xi}^s}}_{c_\mu}\,\kappa^{K-\nu+n+2\mu}\,(1-\kappa)^{\nu-1} \\ \times\quad t^{n+\mu-1}\,a^{\mu+s+1}\,e^{-(t+a)\kappa}\,e^{-a/\bar{\xi}}. \end{aligned} \tag{D.10}$$

Integrating (D.10) with respect to a yields

$$f_{T|\mathcal{K}}(t;\kappa) = \sum_{\mu=0}^{\infty} c_\mu\kappa^{K-\nu+n+2\mu}\,(1-\kappa)^{\nu-1}t^{n+\mu-1}\,e^{-t\kappa}\underbrace{\int_0^\infty a^{\mu+s-1}\,e^{-(kappa+1/\bar{\xi})a}\,da}_{\Gamma(s+\mu)(\kappa+1/\bar{\xi})^{-(\mu+s)}}, \tag{D.11}$$

and a subsequent integration with respect to t gives

$$P_{\mathrm{d}}(\eta)|(\mathcal{K}=\kappa) = \sum_{\mu=0}^{\infty} c_\mu\,\Gamma(s+\mu)\,\frac{\kappa^{K-\nu+n+2\mu}\,(1-\kappa)^{\nu-1}}{\left(\kappa+\frac{1}{\bar{\xi}}\right)^{\mu+s}}\,\underbrace{\int_{\eta}^{\infty} t^{n+\mu-1}\,e^{-\kappa t}\,dt}_{\frac{\Gamma(n+\mu,\kappa\eta)}{\kappa^{n+\mu}}}, \quad \text{(D.12)}$$

and finally after integration with respect to κ and some simple algebra, the detection probability for Test b) becomes:

$$\begin{aligned} P_{\mathrm{d}}(\eta) = \sum_{\mu=0}^{\infty} & \frac{\Gamma(K+1)\Gamma(s+\mu)}{\Gamma(\mu+1)\Gamma(\nu)\Gamma(K-\nu+1)\Gamma(s)}\,\frac{1}{\bar{\xi}^s} \\ \times & \int_0^1 \frac{\kappa^{K-\nu-s}\,(1-\kappa)^{\nu-1}}{\left(1+\frac{1}{\kappa\bar{\xi}}\right)^{\mu+s}}\,\frac{\Gamma(n+\mu,\kappa\eta)}{\Gamma(n+\mu)}\,d\kappa \end{aligned} \quad \text{(D.13)}$$

It is interesting to note that (D.13) looks very similar to the P_{d} of Test a) in (53) except that Test b) requires to integrate over the incomplete gamma-function. The derivation of the special case $s \to \infty$, i.e. the deterministic target scenario, following the analysis in section 4.2.3 and Annex A, is left to the interested reader.

I order to demonstrate that (D.13) is indeed implementable, Fig. D.1 compares the P_{d} of both tests for a given simulation scenario involving a Swerling II target. Please note that the red curve in fact crosses the blue curve indicating that for particular false alarms Test b) can perform better than Test a), which is counterintuitive given that Test a) partly requires the knowledge of $\mathbf{R}$.

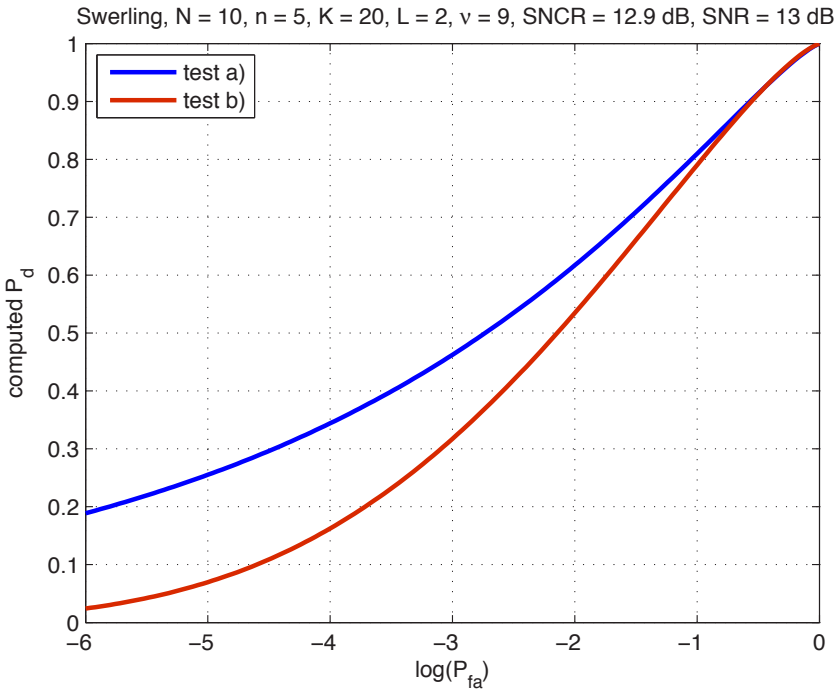

Figure D.1: *Comparison of the ROC of SMI for both tests.*

DOCUMENT CONTROL DATA

(Security classification of title, body of abstract and indexing annotation must be entered when document is classified)

1. ORIGINATOR (The name and address of the organization preparing the document. Organizations for whom the document was prepared, e.g. Centre sponsoring a contractor's report, or tasking agency, are entered in section 8.)

Defence R&D Canada – Ottawa
3701 Carling Avenue, Ottawa ON K1A 0Z4, Canada

2a. SECURITY CLASSIFICATION (Overall security classification of the document including special warning terms if applicable.)

UNCLASSIFIED

2b. CONTROLLED GOODS

(NON-CONTROLLED GOODS)
DMC A
REVIEW: GCEC APRIL 2011

3. TITLE (The complete document title as indicated on the title page. Its classification should be indicated by the appropriate abbreviation (S, C or U) in parentheses after the title.)

On the Receiver Operating Characteristics of Adaptive Radar Detectors

4. AUTHORS (Last name, followed by initials – ranks, titles, etc. not to be used.)

Gierull, C. H.

5. DATE OF PUBLICATION (Month and year of publication of document.)	6a. NO. OF PAGES (Total containing information. Include Annexes, Appendices, etc.)	6b. NO. OF REFS (Total cited in document.)
December 2013	50	33

7. DESCRIPTIVE NOTES (The category of the document, e.g. technical report, technical note or memorandum. If appropriate, enter the type of report, e.g. interim, progress, summary, annual or final. Give the inclusive dates when a specific reporting period is covered.)

Technical Memorandum

8. SPONSORING ACTIVITY (The name of the department project office or laboratory sponsoring the research and development – include address.)

Defence R&D Canada – Ottawa
3701 Carling Avenue, Ottawa ON K1A 0Z4, Canada

9a. PROJECT OR GRANT NO. (If appropriate, the applicable research and development project or grant number under which the document was written. Please specify whether project or grant.)	9b. CONTRACT NO. (If appropriate, the applicable number under which the document was written.)
15eq01	

10a. ORIGINATOR'S DOCUMENT NUMBER (The official document number by which the document is identified by the originating activity. This number must be unique to this document.)	10b. OTHER DOCUMENT NO(s). (Any other numbers which may be assigned this document either by the originator or by the sponsor.)
DRDC Ottawa TM 2013-117	

11. DOCUMENT AVAILABILITY (Any limitations on further dissemination of the document, other than those imposed by security classification.)

(X) Unlimited distribution
( ) Defence departments and defence contractors; further distribution only as approved
( ) Defence departments and Canadian defence contractors; further distribution only as approved
( ) Government departments and agencies; further distribution only as approved
( ) Defence departments; further distribution only as approved
( ) Other (please specify):

12. DOCUMENT ANNOUNCEMENT (Any limitation to the bibliographic announcement of this document. This will normally correspond to the Document Availability (11). However, where further distribution (beyond the audience specified in (11)) is possible, a wider announcement audience may be selected.)

UNLIMITED

13. ABSTRACT (A brief and factual summary of the document. It may also appear elsewhere in the body of the document itself. It is highly desirable that the abstract of classified documents be unclassified. Each paragraph of the abstract shall begin with an indication of the security classification of the information in the paragraph (unless the document itself is unclassified) represented as (S), (C), or (U). It is not necessary to include here abstracts in both official languages unless the text is bilingual.)

Aim of this technical memorandum is to analytically derive the probability of detection (vrs the probability of false alarms) of two variants of a square-law based adaptive radar detector when the target signal is buried in colored interference and when the filter vector to suppress the interference is not constant (i.e. unknown asymptotic covariance matrix) but a random vector itself. The filter or weight vector is assumed to be estimated via either Sample Matrix Inversion (SMI), Loaded SMI (LSMI) or Projection Techniques, such as Eigen-Vector Projection (EVP), Hung-Turner Projection (HTP) or Matrix Transformation based Projections (MTP), based on a limited number of statistical independent secondary training data. The analysis is based on a homogeneous, i.e. Gaussian, stationary clutter plus noise assumption. Target signals comprise different fluctuating RCS models as well as a constant deterministic model. The test statistic provides for the summation of several independent cells ('looks') to improve detection performance whereby the target must not necessarily be present in each cell. Although the analyzed detectors may not directly be applicable, the provided analytical analysis permits an analytical comparison of the various adaptive weights estimation techniques. In this sense it is an extension of the work presented in a previous technical memorandum [1] and its results and conclusions reflect an intermediate step towards unifying quantitative assessment of more advanced detectors such as the Adaptive Matched Filter (AMF) among others. The capability and usefulness of the presented equations are demonstrated based on numerical examples with a variety of different radar parameter settings.

14. KEYWORDS, DESCRIPTORS or IDENTIFIERS (Technically meaningful terms or short phrases that characterize a document and could be helpful in cataloguing the document. They should be selected so that no security classification is required. Identifiers, such as equipment model designation, trade name, military project code name, geographic location may also be included. If possible keywords should be selected from a published thesaurus. e.g. Thesaurus of Engineering and Scientific Terms (TEST) and that thesaurus identified. If it is not possible to select indexing terms which are Unclassified, the classification of each should be indicated as with the title.)

Synthetic Aperture Radar; Ground Moving Target Detection; Probability of False Alarms; Probability of Detection; Sample Matrix Inversion (SMI); Receiver Operating Characteristics

Defence R&D Canada

Canada's leader in Defence
and National Security
Science and Technology

R & D pour la défense Canada

Chef de file au Canada en matière
de science et de technologie pour
la défense et la sécurité nationale

www.drdc-rddc.gc.ca